Griffith UNIVERSITY
Queensland, Australia

Noise in MEMS

Author

Mohd-Yasin, F, Nagel, DJ, Korman, CE

Published

2010

Journal Title

Measurement Science and Technology

DOI

https://doi.org/10.1088/0957-0233/21/1/012001

Copyright Statement

© 2010 Institute of Physics Publishing. This is the author-manuscript version of this paper. Reproduced in accordance with the copyright policy of the publisher.Please refer to the journal's website for access to the definitive, published version.

Downloaded from

http://hdl.handle.net/10072/37717

Griffith Research Online

https://research-repository.griffith.edu.au

TB, SB, US, MST/256780, 2/09/2009

IOP PUBLISHING MEASUREMENT SCIENCE AND TECHNOLOGY

Meas. Sci. Technol. **20** (2009) 000000 (22pp) UNCORRECTED PROOF

TOPICAL REVIEW

Noise in MEMS

F Mohd-Yasin[1], D J Nagel[2] and C E Korman[2]

[1] Faculty of Engineering, Multimedia University, 63100 Cyberjaya, Selangor, Malaysia
[2] Department of ECE, The George Washington University, Washington, DC 20052, USA

Received 06 August 2007, in final form 06 July 2009
Published DD MMM 2009
Online at stacks.iop.org/MST/20/000000

Abstract
This review provides a comprehensive recap of noise research in MEMS. Some background on noise and on MEMS is provided. We review noise production mechanisms, and highlight work on the theory and modeling of noise in MEMS. Then noise measurements in the specific types of MEMS are reviewed. Inertial MEMS (accelerometers and angular rate sensors), pressure and acoustic sensors, optical MEMS, RF MEMS, surface acoustic wave devices, flow sensors, and chemical and biological MEMS, as well as data storage devices and magnetic MEMS, are reviewed. We indicate opportunities for additional experimental and computational research on noise in MEMS.

Keywords: noise, MEMS, micro systems

1. Introduction to noise

Noise is an area of science and technology, which poses practical problems, but also has deep intellectual attractions. The diverse mechanisms and magnitudes of noise challenge both their understanding and control. There are two fundamental and inescapable reasons for noise in electrical and other systems. One is the quantization of basic physical entities, such as electrons, atoms and molecules. The other is their large numbers of such units in most situations, and the inevitable variances in the number of entities. The energies associated with particles, photons and other quanta also have unavoidable distributions. Systems with small numbers of discrete units can be handled deterministically. Other systems with large numbers of discrete units, such as vehicular traffic, are intermediate between deterministic and statistical. But electronic and other systems have such large numbers of quanta that only statistical treatments are tenable for manageable description of device behavior.

Noise includes both unavoidable noise intrinsic to the system being used and extrinsic noise that might be ameliorated by shielding or other means. The problems caused by noise are well known. They fall into two categories. The first is degradation of performance. The decline in fidelity of the output of an acoustic system, such as a speaker, is a familiar example. In general, the quality of the output of any actuator, which turns information into a physical, chemical or biological effect, can be negatively impacted by noise.

The second deleterious result of noise is to degrade or limit the output of sensors or measurement systems that turn any of the external effects into information. Virtually all such systems have a calibration curve, as shown schematically in figure 1. Calibration curves relate what is being measured, the measurand M, to the signal S from the sensor or system. The slope $\Delta S/\Delta M$ is the responsivity of the sensor. The useful range is capped on the high end by saturation of some part of the system. Noise limits how small a value of the measurand can be detected reliably. That is, noise determines the limit of detection (LOD), which is also called the minimum detectable limit (MDL), of the measurand for some particular measurement situation.

Much attention has been given to the LOD of analytical and other measurement systems. Sometimes, the LOD is simply taken as the value of the measurand at which the mean signal is 3σ above the mean of the noise values. Here, σ is the standard deviation of the distribution of the noise values obtained over time. Alternatively, 'receiver operating characteristics', called ROC curves, are employed for more precise but more complex determination of the tradeoffs involved in determining the LOD. ROC curves permit rational choices of the number of false positives that can be tolerated for a given situation and sensor system.

 © 2009 IOP Publishing Ltd Printed in the UK

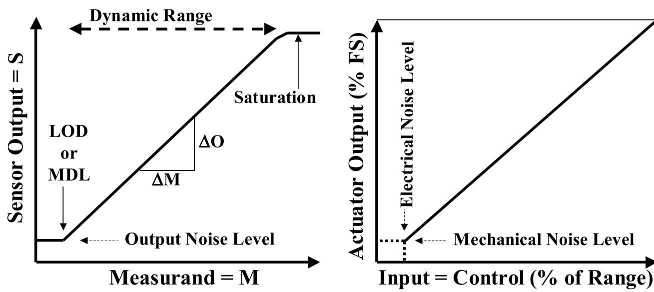

Figure 1. Left: schematic of a calibration curve for a sensor or an analytical instrument. Calibration curves need not be linear over their dynamic ranges, as shown here. Both axes can be either linear or logarithmic. Right: schematic of the control curve for an actuator. Control curves are often nonlinear and sometimes hysteretic, in which case the output for a given input can be double valued. The axes for control curves of actuators are generally linear.

Noise can also limit the output of MEMS and other actuators at low values of the input (control) signals, as shown in figure 1. Control curves relate the electrical input, which varies over some range, to the mechanical output, which is full scale (FS) at 100% of the input value. For sensors, the measurand is often stable (not noisy), although the position of what is being measured can be noisy for mechanical sensors. For MEMS actuators, the performance can be limited by either electrical input or mechanical output noise.

In short, the performances of both types of transducers, sensors and actuators of any size, can be degraded by noise. Such problems can be especially acute for MEMS transducers because of the relatively small sizes of these devices and their electronic, mechanical and other parts.

2. Introduction to MEMS

MEMS sensors and actuators are devices that have static or movable components with some dimensions on the scale of a micrometer. Micromachined sensors and actuators commonly combine the electronic, mechanical, optical, magnetic or other components in a single chip (Nagel and Zaghloul 2001). MEMS is a well-established field, which has its roots in the 1960s and it is still evolving rapidly. Today, hundreds of MEMS components are being used in a broad range of applications. MEMS devices, especially sensors, are now sold by the tens of millions annually. Pervasive ownership and use of MEMS are becoming normal.

The annual revenues for MEMS sensors and actuators are predicted by Yole Development to exceed 10 billion USD during 2010. MEMS transducers are expected to dominate some markets eventually due to the three advantages over conventional sensors and actuators, namely high performance, low cost and low power.

MEMS-based accelerometers and pressure sensors in automotive and other industries have proven to be very successful applications. Furthermore, RF MEMS and optical MEMS are increasingly being adopted in telecommunication systems. Due to these commercial successes, the research and development of MEMS are actively being pursued around the world, especially in the USA, Germany and Japan. Substantial numbers of journals and conferences have been dedicated to this particular field. Various reference books are dedicated to this topic (Korvin and Greiner 2002, Maluf 1999, Senturia 2000, Kovacs 1998, Rebeiz 2002a, Pelesko and Bernstein 2002, El-Haks 2001, Santos 2002). Moreover, patents on MEMS are now granted at a global rate of exceeding one per work-day.

3. Overview of this review

In general, the role of noise in MEMS has two aspects, similar to noise in any devices. The first is the existence of various noise sources, while the second is the practical limitations that noise places on a MEMS system. Due to the diversity of MEMS, there are many noise sources, depending on the physical and other characteristics of the sensors and actuators. For example, the noise sources in a mechanical system can be different than the noise sources in optical, magnetic or fluidic systems. Moreover, most micro systems involve two or more physical or other characteristics, such as optical MEMS, which have electrical, mechanical and optical mechanisms, all tightly integrated.

It is well known that noise is the limiting performance factor in many systems. Before the introduction of MEMS, there was less need to closely examine the influence of noise for many devices, because vibration or other instabilities generally came from external sources (Talghader, 2004). However, the development of MEMS has changed this balance between the extrinsic and intrinsic noise. Due to the miniaturization, the interaction of noise energy with an extremely small mass can cause distortion that will affect the performance of a micro system, opening opportunities for the study of noise from new perspectives. For example, the mechanical–thermal noise is not a new concept, but its effects were rediscovered when MEMS sensors were pushed to the limits of their performance.

MEMS sensors and actuators all involve some mechanisms and associated microstructures. Common mechanisms are capacitive, piezoelectric, piezoresistive and tunneling. Several types of MEMS work using alternative mechanisms. Pressure sensors, for example, can operate on capacitive, piezoresistive, interferometric and other mechanisms. The noise to which the different mechanisms are subject varies widely. MEMS structures include cantilevers, beams, membranes and inter-digitated (comb) electrodes, among others. These structures also have diverse susceptibilities to different types of noise. There is no obvious way to categorize the subject of noise in MEMS. We chose to organize this review by the types of MEMS devices, because they tend to be closely coupled to the kinds of applications. However, the different types of MEMS can have many distinct applications. Accelerometers are a good example, since they are used in automobiles, toys, cell phones, cameras and laptop computers.

This review provides a comprehensive recap of mostly experimental studies of noise in MEMS. The next section gives some background information on noise sources. A brief section on theory and modeling of MEMS noise follows. A similar short section on techniques for the measurement of

noise from MEMS devices is provided next. Then, we survey noise in some broadly useful MEMS structures. The core of this review consists of summaries of experimental studies, the state of the art of noise measurements, in specific types of MEMS devices. They include accelerometers, angular rate sensors, pressure sensors, microphones, optical MEMS, RF MEMS, SAW devices, flow sensors, chemical sensors, biosensors, data storage devices and magnetic MEMS. Finally, our conclusions and recommendations are presented, one of which deserves highlighting, namely the interactions of noise mechanisms in micro- and nano-scale devices.

A primary challenge in simulating and designing MEMS devices is the close coupling between electrical, mechanical, optical and other mechanisms active in almost all MEMS devices. It is not possible to achieve a proper MEMS simulation or design without taking account of all the relevant mechanisms and their influence on each other. For example, the motion of electrons induces mechanical forces, and deflections cause changes in charge distributions. A fundamental question concerns the coupling of the noise that accompanies the various physical or other mechanisms active in any one MEMS device. That is, does the presence of electronic noise, say Johnson (thermal) noise, influence mechanical (Brownian) noise, which can affect the very small masses in MEMS devices, and vice versa? Similarly, thermal adsorption and desorption noise is mechanical on a molecular level, but can involve electronic effects, when ions are involved. The nature and strengths of the various possible interactions of noise mechanisms remain open research questions, both theoretically and experimentally.

The units with which noise in MEMS and other devices are quantified are numerous and often relatively complex. Several noise units were employed in the studies we review. Hence, we provide an appendix, which surveys and discusses units for noise.

4. Noise sources

Noise has many meanings, so it is necessary to identify the types of noise of interest in this review. Noise in components such as MEMS, and in systems containing them, has two fundamental origins, one external (extrinsic) and the other internal (intrinsic). Noise from outside of MEMS devices due to ambient electromagnetic fields or mechanical motions, notably sound and vibration, can limit the performance of a system. However, external noise sources are not within the scope of this review. The magnitude of external noise signals coupled into a MEMS device varies with the local conditions, that is, the ambient electronic and mechanical environment, and it also depends on the packaging and mounting of the MEMS device. Our focus is on the fundamental noise sources within MEMS devices because they provide the hard limits on the device performance. The reduction of intrinsic noise from various basic mechanisms is an important challenge to the MEMS designer.

Before enumerating some of the more widespread and important noise sources in MEMS, it is useful to reconsider the fundamental causes of noise, in general. Noise in engineering systems has two root causes. The first is the granularity of the energy and matter in devices. Photons, electrons, atoms and molecules are quanta. Their existence within or impact onto devices is unavoidably discrete. The second reason for appearance of noise is the unavoidable statistical variations in the energies and motions of the large numbers of the relevant quanta. In large systems, the discrete and statistical nature of the presence and motions of energy and matter is often negligible. As the size of the systems decrease, signals tend to decrease and subsequently, the noise tends to increase on a relative scale. Together, this has double impacts on the signal-to-noise ratios (SNR). Practical limits on the minimum detection limits of MEMS sensors, and on the minimum required input signals for MEMS actuators, are both set by noise levels. Besides providing engineering limits on the performance of MEMS devices, noise is a complex intellectual subject. This is true for individual noise mechanisms operating within a particular MEMS structure. The subject of interactions between noise mechanisms is even more complex, when there are multiple types of energies in a MEMS device, usually electrical and mechanical, but also optical, radio frequency and others.

There are discussions of many types of noise in the following sections. In the rest of this section, we provide terse summaries of the character of several of these mechanisms. There is one noise mechanism that cuts across most types of MEMS, namely shot noise. It is due precisely to the quantized character of the signals and materials in MEMS. Shot noise is caused by the variable (random) arrival times of electrons or photons, or the necessarily discrete motions of atoms or molecules within or onto a MEMS device.

Electronic noise is most broadly important in MEMS because of the inevitable electronic character of both MEMS sensors and actuators. There are a few electronic noise mechanisms, which receive most attention. They are as follows.

- Thermal (Johnson or Nyquist) noise, which is due to temperature-induced fluctuations in carrier densities (as well as in the motions of atoms and molecules).
- Generation–recombination noise, which is caused by random production and annihilation of electron–hole pairs in semiconductors. It can also appear in and after the ionization due to the absorption of energetic quanta.
- Flicker noise, which varies inversely with frequency ($1/f$), and is due to variable trapping and release of carriers in any conductors. Different types of flicker noise occur in diverse systems of widely varying characters and size scales (Bak 1996).

Mechanical noises, such as microphonics and vibrations, are commonly extrinsic. However, there is one fundamental intrinsic mechanical noise mechanism, namely Brownian motion. It is due to the dynamic unbalanced forces caused by random impacts of molecules on a small particle or structure. Hence, it is also called 'random walk' noise. Brownian motion becomes more significant as the size of a structure decreases, for example, the proof mass in a MEMS accelerometer or a resonant beam in a MEMS RF filter. Adsorption–desorption noise is closely related to Brownian motion. It is due to

Table 1. Papers reporting on theory and modeling of MEMS noise.

Paper	Device or structure	Focus	Characterization
Gabrielson (1993)	Accelerometers, pressure sensors, capacitive microphones	Mechanical–thermal noise	Theory
Djuric (2000)	Accelerometers, infrared thermal detectors, micro-beams	Several mechanisms	Theory
Djuric *et al* (2002)	Microcantilevers and micro-resonators	Several mechanisms	Theory and computations
Greiner and Korvink (1998)	Micro bars	Mechanical noise	Theory
Vig and Kim (1999)	Resonators (micro-beams)	Several mechanisms	Theory and computations
Leland (2005)	Gyroscopes	Mechanical–thermal noise	Theory

the random arrival and departure of individual atoms and molecules on the surface of a MEMS device. Adsorption–desorption noise involves some non-zero particle residence time on a surface, in contrast to the transient impacts that cause Brownian motion. It is a common problem in chemical and biological sensors, which contain small structures.

An important type of noise in an optical beam is noise in its intensity. It results from quantum noise (associated with laser gain and cavity losses), partly from sources such as excess noise of the pump source, vibrations of cavity mirrors or thermal fluctuations in the gain medium. The resulting relative intensity noise (called RIN) also depends on the operation conditions. In particular, it often becomes weaker at high pump powers, where the relaxation–oscillations are strongly damped.

In the RF domain, an ideal carrier would appear as an infinitesimally thin line in a frequency spectrum. The typical carrier, however, will have skirts whose amplitudes roughly follow $1/f$ distributions for frequencies relative to and away from that of the carrier. These skirts are the envelope of sidebands due to modulations of the carrier, and are FM and AM in nature, random in both frequency and amplitude, and caused by various phenomena relating to the physics of the particular oscillator. They are commonly referred to as phase noise. Phase noise is typically expressed in units of dBc Hz^{-1} at various offsets from the carrier frequency. dBc is the noise intensity relative to the carrier strength. Phase noise can be measured and expressed as SSB (single sideband) or DSB (double sideband) values.

Granularity in magnetic media produces zigzag transitions of their magnetic polarizations. The exact locations of the zigzags change from write to write, causing media noise (also known as transition noise or zigzag noise). It has become the dominant noise source in modern disk drive channels.

It must be noted that presenting and discussing the many equations that relate the amount of each type of noise to the governing parameters, especially temperature, are beyond the scope of this review. The authors refer readers to the works of Gabrielson (1993), Djuric (2000), Kulah *et al* (2006), Yeh and Najafi (1997), Seshia *et al* (2002) and Cleland and Roukes (2002). These papers contain the expressions for computing the magnitude of contributions from various noise mechanisms in several MEMS devices.

Q1

In reading papers on noise, one encounters the concept called ‘input referred noise’. It refers to representing the effect of all of the noise sources in an amplifier circuit by noise sources at the input, which would produce output noise equal to the actual output noise. That is, the fictitious ‘input referred noise’, multiplied by the gain of an amplifier, equals the actual output noise. The idea is to enable a fair comparison of the noise introduced by an amplifier. This ‘noise’ is may be due to the effects of several mechanisms in diverse components within the amplifier. Hence, like ambient noise, it is not of interest for this review.

This summary of the noise sources in electrical, mechanical, optical, RF and magnetic MEMS is not comprehensive. For example, we did not address thermal conductance noise, which is due to fluctuations in the heat conductivity of pixels in MEMS infrared detector arrays. However, the more general noise sources cited above provide backgrounds for most of the specific noise studies that are discussed in the following sections. Next, we review briefly some of the theoretical, analytical and computational work on noise in MEMS.

5. Theory and modeling

Substantial work has been done on the theory and modeling of MEMS noise. Table 1 is a summary of the selected works being highlighted in this review. The most notable work is by Gabrielson (1993), who published a paper that discussed the effects of mechanical–thermal noise for MEMS, which is the basis of much subsequent work. He reviewed several techniques for calculating the mechanical–thermal noise in simple MEMS structures, such as mass-spring accelerometer, pressure sensor, capacitive microphone and electron tunneling accelerometer. In this 1993 paper, Gabrielson used Nyquist’s relation to give the spectral density of the fluctuating force related to any mechanical resistance, which is a direct physical analog of Johnson noise related to electrical resistance. It is given in the equation

$$F_{\mathrm{mechanical-thermal\ noise}} = \sqrt{4k_{\mathrm{B}}TR}\,\mathrm{N(Hz)}^{-1}, \quad (1)$$

where k_{B} is the Boltzmann constant, T is the absolute temperature and R is the mechanical resistance, or most commonly known as a damping coefficient. To date, Gabrielson’s paper had been cited more than 300 times. It remains as the most referenced paper on noise in MEMS.

One follow-up study was performed by Djuric (2000) who derived more complex noise models. He combined

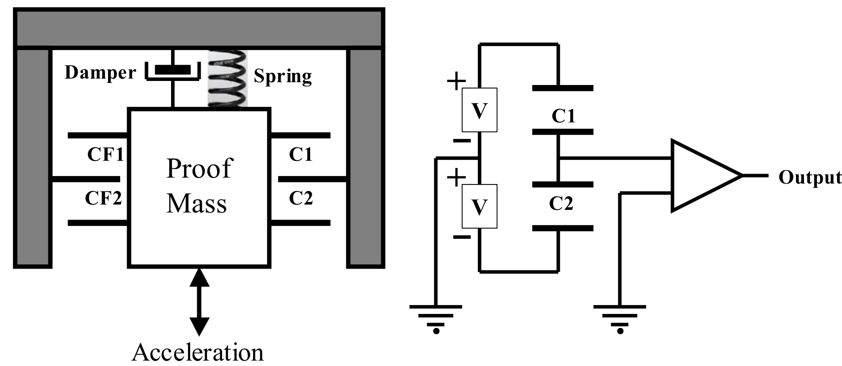

Figure 2. Schematic diagram for a MEMS accelerometer with a differential capacitance as the means of detecting motion of the proof mass relative to the frame (gray). A simple capacitance bridge is used to detect the motion-induced capacitance differential between C1 and C2. A force feedback unit, consisting of two capacitors (CF1 and CF2), holds the mass near its undeflected position in order to broaden the dynamic range (voltages on CF1 and CF2 are not shown). Mechanical noise can affect the mass and electronic noise the circuit (after Djuric 2000).

mechanical–thermal noise with electrical noise sources, such as shot noise, thermal noise and $1/f$ noise in the improved model. The equations for some of the most common electrical noise sources are given below:

$$V_{\text{thermal noise}} = \sqrt{4kTBR}, \tag{2}$$

where B is the measurement bandwidth and R is the electrical resistance;

$$I_{\text{shot noise}} = \sqrt{2qI_{\text{dc}}B} \tag{3}$$

where q is the electron charges (1.6×10^{-19} Coulombs), I_{dc} is the average direct current (A) and B is the noise bandwidth (Hz); and

$$I_{\text{flicker noise}} = \sqrt{\frac{KI_{\text{dc}}B}{f}}, \tag{4}$$

where I_{dc} is the average value of direct current (A), f is the frequency (Hz), K is a constant that depends on the type of material and its geometry.

The results were used to calculate the performance limitation of accelerometers, sensing probe cantilevers and thermal infrared detectors. Figure 2 shows the model of a capacitive accelerometer and the associated circuit. It is a schematic diagram of a MEMS accelerometer with a differential capacitance means of detecting the relative motion of the proof mass due to inertia. The device illustrated uses force feedback to maintain the position of the mass near its position for zero acceleration.

In another work, Djuric *et al* (2002) derived the equivalent noise model for a microcantilever. The study found adsorption–desorption processes, temperature fluctuations and Johnson noise as the dominant noise sources in microcantilevers at high frequencies, whereas the adsorption–desorption noise dominated at low frequencies.

Another similar study extracted noise parameters for the macro-modeling of MEMS (Greiner and Korvink 1998). The work investigated the noise sources in the mechanical energy domain, where the noise was described by a correlation function under different operating conditions. The correlation functions of the different dissipation channels were developed using a vibrating micro bar as a practical example.

One theoretical study of noise in MEMS-based resonators was done by Vig and Kim (1999). The work discussed the stability of resonators as the dimensions of the devices become smaller. It was observed that, with decreasing dimensions, the relative instabilities increased, which caused devices to fluctuate. Further investigation revealed that the fluctuations were caused by temperature, adsorption–desorption of molecules, out gassing, Brownian motion, drive power, self-heating and random vibration. The authors derived the equation for the noise of micro- and nano-resonators due to temperature fluctuations. Q2

Another theoretical work on noise in MEMS focused on the micro gyroscope (angular rate sensor). Leland (2005) derived expressions for the effect of mechanical–thermal noise on a vibrational gyroscope, including the angular random walk, the noise-equivalent rotation rate and the spectral density of the noise component of the rate measurement. He calculated and compared the output due to rotation and the output due to noise, using stochastic averaging to obtain an approximate 'slow' system. The paper clarifies the impact of thermal noise and shows the effect of frequency mismatch between the drive and sense axes. The noise-equivalent rates for both open-loop and force-to-rebalance operation of the gyroscope were also found.

6. Measurement techniques

In general, a noise measurement system consists of device under test (DUT), low-noise amplifier, spectrum analyzer and computer for data plotting and analysis. Figure 3 shows the typical noise measurement for MEMS inertial sensors. The noise voltage output from the DUT is fed to the low-noise amplifier (LNA), which is used as a front-end amplifier. The LNA amplifies the noise voltage without adding significant noise, and then the amplified noise voltage is fed into the spectral analyzer. The analyzer measures the power spectrum of the noise signal and displays the results on logarithmic scale such as dBm. In most modern measurements, data from the analyzers are fed to the personal computer via a GPIB cable for analysis.

Figure 4 shows a method used to measure SAW resonator phase noise (Enguang 2002). In this setup, a phase bridge

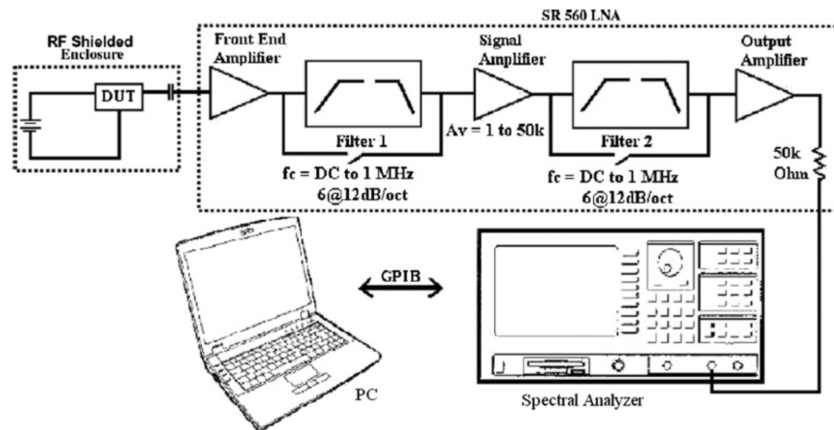

Figure 3. Typical setup of a low-frequency noise measurement system (Mohd-Yasin *et al* 2009).

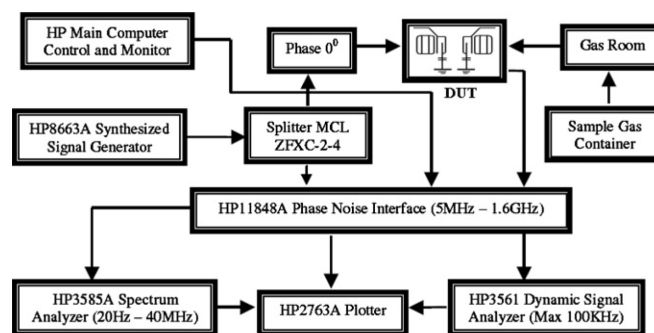

Figure 4. Setup to measure phase noise from surface acoustic wave devices (Enguang 2002). The HP 11484A is the phase bridge referred to in the text.

is used to differentiate the phase of two signals, namely the referenced signal and the measured signal coming from the SAW resonator (DUT). The HP8663 A synthesizer provides the low-noise carrier signal which is split into two signals. The first half acts as a referenced signal that goes to the one arm of the phase bridge. The second half of the signal is injected into the input of the two-port SAW resonator (DUTs). The DUT is mounted on a chamber filled with sample gas that would cause frequency shift at the output of the resonator. The output signal is then fed to another arm of the phase bridge. The lengths of the DUT and non-DUT signal paths connected to the phase bridge are adjusted to obtain the phase quadrature at the phase detector, which is then fed to HP11848 A phase noise interface unit. The data are copied by the HP2763 A plotter, and the phase noise is displayed on the HP3585 A spectrum analyzer or the HP3561 dynamic signal analyzer.

An example of the setup to measure the noise amplitude of a chemical sensor is shown in figure 5 (Hoel *et al* 2002). In this work, an Au thin film was coated with tungsten trioxide, which produces conductance noise at the output of the sensor. A four-point measurement setup with a dc current generator was used to detect the signal fluctuations, shown in part (*a*). The voltage fluctuations represent the resistance, which is the conduction noise of the sensor. The amplitude of the fluctuation is proportional to the amplitude of the noise. The measurement was ac coupled to the input of the FET differential amplifier, which amplified the signal to 80 dB, and converted it to digital data with an NI 16 bit ADC. The data were fed to the PC for further processing. An FFT was performed to obtain the noise spectra from 0.5 to 30 kHz.

7. Common MEMS structures

The field of MEMS involves some characteristic and broadly applicable microstructures, which can be used in a variety of applications. Examples are cantilevers and other types of resonant micro-mechanical structures. Structures with varying capacitance, due to the motion of facing plates or inter-digitated parts, are common in many devices. The few, quite recent studies of noise in these widely useful structures are surveyed in this section.

Microcantilevers are especially useful in diverse MEMS sensors, most notably as the active element in atomic force microscopes (AFM) for imaging surfaces with atomic resolution and for manipulating molecules on surfaces. They have also been shown to be useful for measuring accelerations, as the active element in radio-frequency switches, as part of micro-fluidic systems and for mass and bio-chemical sensing.

Both commercial cantilevers and research structures have been employed in MEMS noise studies. McLoughlin *et al* (2007) measured the power spectral distribution (PSD) of AFM cantilevers immersed in solutions of poly(ethylene glycol) over temperatures of 23–33 °C. Optical reflectivity means of measuring displacements were employed with a spectrum analyzer to record noise spectra. The data were used to

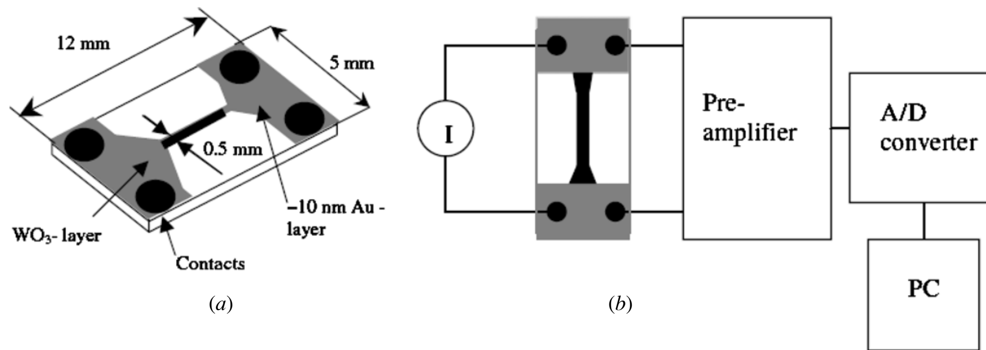

Figure 5. (*a*) A schematic perspective view of a noise sensor device. (*b*) Electronic setup to measure the noise (Hoel *et al* 2002).

obtain the numerical values of the density and viscosity of the fluids, which compared well with values from the literature that were measured using macroscopic instruments. The work opens the possibility of measuring fluid properties with very small samples, possibly in micro-fluidic systems. Specially fabricated doped silicon microcantilevers were used by Lee *et al* (2008) to obtain resonance behavior and noise spectra in the range of 25–175 °C. Both local and uniform heating were employed. For the geometries used, local heating had a greater effect on changes in the resonance frequency of the cantilevers. The key point from such studies and other applications of microcantilevers is the fact that thermally induced, noisy motions can be exploited for applications or used to modify the mechanical behavior of the structures.

Resonant MEMS structures, besides cantilevers, are also widely useful. They can range from simple beams clamped on both ends to complex structures with inter-digitated fingers that are suspended on springs. Depending on the size and ambient atmosphere, such structures are subject to thermo-mechanical noise, including Brownian motion and absorption–desorption noise. In one recent study, Sharma *et al* (2008) did an analysis and optimization for noise in MEMS resonant structures. They compared finite element calculations with parametric expressions for squeezed-film damping obtained from analytical models. This permitted extraction of a behavioral model for the resonant vibratory 'gyroscope', that is, an angular rate senor based on the Coriolis force. Both thermo-mechanical and electronic noises were taken into account. There is great room for additional studies of noise in resonant structures.

The following sections deal with the various types of noise measured in the different classes of MEMS, which have various applications. The specific microstructures and noise measurement techniques used to obtain the results, which are reviewed, can be found in the references.

8. Accelerometers

MEMS accelerometers are the most mature product among inertial MEMS. Major markets for MEMS accelerometers are automobile airbag triggers, earthquake detection circuits, health care, toys, cameras and cell phones. Since MEMS accelerometers are used in many systems, the noise characteristics of these devices are important. They limit the performance of systems, especially when operating under low acceleration conditions.

Three groups in Japan, the USA and Holland have modeled and characterized noise of custom-made capacitive micro-accelerometers. The Japanese group used a linear noise model to simulate and measure the thermal–mechanical and input-referred noise characteristics for a capacitive-servo accelerometer (Yoshida *et al* 2005). University of Michigan researchers constitute one of the leading groups in designing ultrasensitive micro-accelerometers that are able to detect micro-g (gravity) levels (Kulah *et al* 2006). They discovered that the mechanical noise is generally dominant, and therefore designed the sensor structure with large proof mass and small damping factor. The third work by the Dutch group attempted to characterize directly the mechanical–thermal noise spectrum by repeatedly bringing the capacitive micro-sensor to pull-in, and measuring the pull-in time, followed by an FFT (Rocha *et al* 2005). They found that the white noise level is in agreement with existing theory on damping, and that the $1/f$ noise is independent of the ambient gas pressure.

Oropeza-Ramos *et al* (2008) performed the noise analysis of a tunneling accelerometer. The custom device had been fabricated with a low-noise differential transresistance amplifier with a large gain. The dynamic model of the closed loop system was constructed using stochastic control theory. Thermo-mechanical noise from the proof mass motion, shot noise from the tunneling junction and Johnson resistor noise were considered. The analysis was based on a linearized model, similar to the approach of Yoshida *et al* (2005). They found a 30% difference between the theoretical and experimental standard deviations of the tunneling signal, which was attributed to the inaccuracies of the work function (Φ) in the tunneling model.

The author's group performed a study of noise in commercial MEMS accelerometers (Mohd-Yasin *et al* 2003, 2007, 2008). The noise spectrum was measured as a function of the acceleration of gravity in the range from −1 to +1 g. A common spectral behavior of noise was found, with approximately $1/f$ noise dominating at low frequencies and white thermal noise being the limiting factor at higher frequencies. Unexpected resonances were also observed in three commercial devices. Figure 6 shows the noise characteristics for ADXL105 from analog devices. They were measured with the setup shown in figure 3.

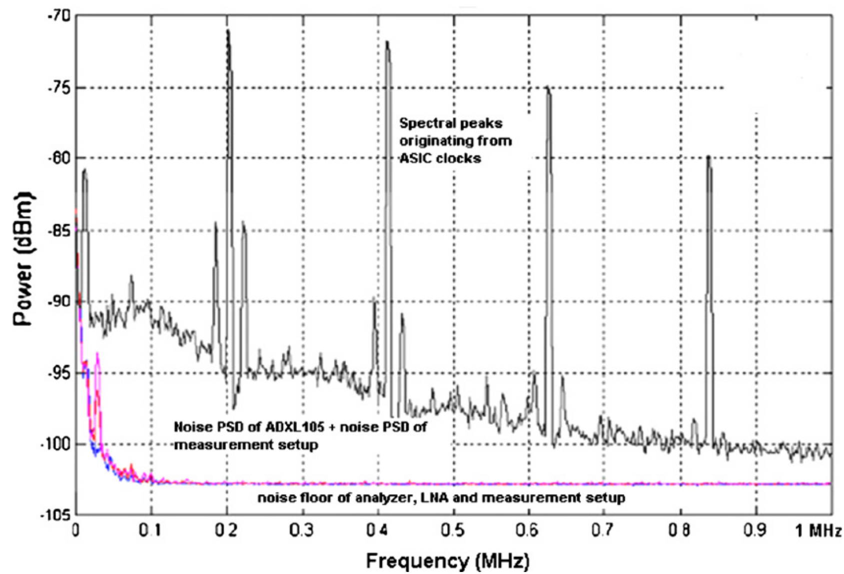

Figure 6. ADXL105 noise characteristics at zero gravity (Mohd-Yasin *et al* 2008). The peaks are due to the harmonics of the oscillator inside the chip, and are not noise.
(This figure is in colour only in the electronic version)

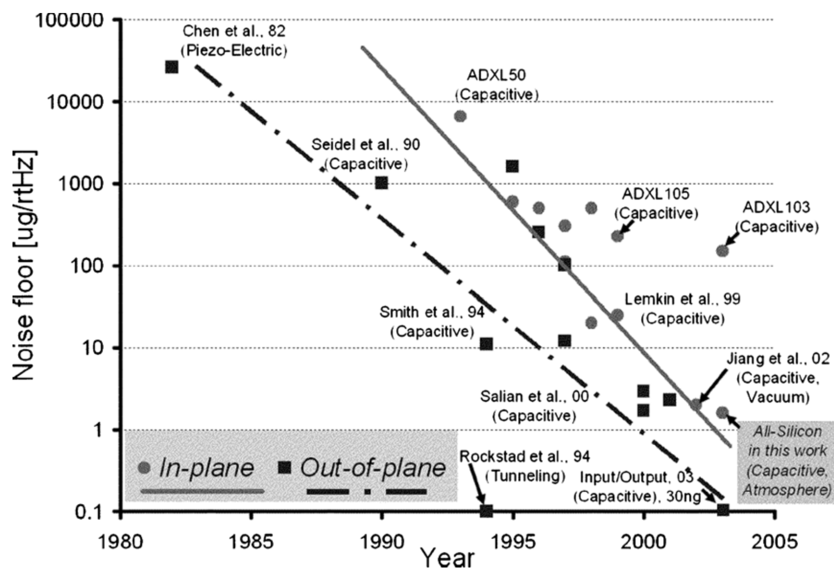

Figure 7. Performance of micro-accelerometers in term of noise floor versus year (Chae *et al* 2004).

Apart from noise measurements of MEMS accelerometers, several designers have used noise theory to increase the sensitivity of their sensors. The most prominent group is led by Professor Najafi from University of Michigan. In Yazdi and Najafi (2000), the modeling and noise analyses of closed-loop micro-g accelerometers with deposited rigid electrodes were performed. This work identified several types of noise sources that affect micro-accelerometers, such as mechanical noise, thermal noise, amplifier noise, sensor-charging reference voltage noise, clock jitter noise and quantization noise. Chae *et al* (2004) produced a nice summary of the progress in developing low-noise micro-accelerometers, as shown in figure 7.

Noise modeling and analysis were also performed with tunneling accelerometers (Liu and Kenny 2001, Yeh and Najafi 1997), automotive accelerometers (Joseph *et al* 1996) and resonant micro-accelerometers (Seshia *et al* 2002). All these studies focused on accelerometer's noise characteristics under static conditions. However, two works were able to study noise characteristics under dynamic conditions. In Han and Cho (2003), the performance of an accelerometer and its noise characteristics were recorded with varying voltages and pressures. In Liu *et al* (1998), a shake table was used to create dynamic accelerations to measure noise and other characteristics of a tunneling accelerometer. In addition to the noise research mentioned above, there are many works that used noise theories to optimize accelerometer designs (Boser and Howe 1996, Yazdi *et al* 2003, Yeh and Najafi 1997, Kajita *et al* 2002, Monajemi and Ayazi 2006, Amini and Ayazi 2005).

9. Angular rate sensors

MEMS 'gyroscopes', more accurately known as angular rate sensors, have increasingly taken the place of conventional rate sensors in many applications. There are three primary works that investigated the noise properties of a MEMS gyroscope. The first studied the effect of mechanical–thermal fluctuations on a vibrating-mass surface-micromachined gyroscope (Annovazi-Lodi and Merlo 1999). It was found that the mechanical–thermal noise source represents a practical sensitivity limit in the gyroscope and is likely to restrict their performance, even in automotive applications that do not require high sensitivity. The study concluded that the vibrating-mass surface-micromachined gyroscope structure would require a significant dimension increase or a completely different design to increase the sensitivity and lower the noise floor. The second work extended the first by considering the effect of the angular random walk, the noise-equivalent rotation rate and the spectral density of the noise component of the rate measurement (Leland 2005). The third paper (Lin and Stern 2002) analyzed the behavior of a DSP-based correlation filter used to mitigate the effects of thermal noise in a low-cost MEMS gyroscope. It discusses the mechanical thermal noise and its simulated effect on the performance of the gyroscope.

Many gyroscopes designers take into consideration the noise factor to improve the performance of their designs. The earliest work is by Degani *et al* (1998) that derived the noise-equivalent rate (NER) of a rate gyroscope, among others including the mechanical behavior, optical sensing and electronics in order to derive an optimal design approach for his design.

Designers have also utilized different types of sensing mechanisms such as tuning forks, oscillating wheels, Foucault pendulums and 'wine glass' resonators to obtain angular rates. In all cases, noise is one of the main factors that has been taken into the design consideration. Three works (Seshia *et al* 2002, Xie and Fedder 2003, Shcheglov *et al* 2000) discussed the effects of electrical–thermal noise in a resonant-output gyroscope, a deep-reactive-ion-etch (DRIE) CMOS gyroscope and a jet propulsion lab (JPL) gyroscope. The last work on the JPL gyroscope concentrated on the effect of noise at high temperature because of its intended applications in aerospace.

The latest work from University of Berkeley attempted to reduce the effect of electrical noise from the interface circuitry of inertial sensors (Petkov and Boser 2005). In addition to all the studies mentioned above, there is one practical study (Palaniappan *et al* 2003), which compared several key parameters such as noise floor of two different integrated surface micromachined z-axis frame-gyroscopes that were fabricated on the same chip.

10. Pressure sensors

Along with accelerometers, pressure sensors are a main commercial success of MEMS. They generally measure low-bandwidth pressure variations. Interestingly, there are few studies of noise in low-frequency pressure sensors. One project integrated a piezoresistive pressure sensor with ring oscillator readout on the same chip in an effort to reduce noise (Oysted and Wisland 2005). A theoretical and computational study of noise in MEMS pressure sensors compared the performance of three readout mechanisms (Pattnaik *et al* 2005). It was found that the noise-equivalent pressure for a guided wave optical pressure sensor was much smaller than for either capacitive or piezoresistive readouts. Clearly, there are many opportunities for experimental noise studies in MEMS pressure sensors with diverse readout mechanisms.

11. Microphones

Microphones are devices to measure high-frequency pressure variations, that is, audible and ultrasound signals. There are several studies of noise in microphones. In many MEMS acoustic sensors, the amplitude of input-referred (or electronics) noise of the attached preamplifier stage is much larger than the noise from within the sensors. In such cases, the electronics noise is the dominant source with a high acoustical equivalent input noise. In other devices, thermo-mechanical noise from inside a microphone dominates.

Numerous studies were performed to investigate the noise properties, and most importantly, to optimize the SNR in acoustic sensors. Five research papers are reviewed next. The earliest was performed by Gabrielson (1995), when he studied the fundamental noise limits for miniature acoustic and vibration sensors. The paper reviewed several techniques for evaluating noise in acoustic and vibration sensors, in general, and in micromachine sensors, in particular, taking into considerations three factors. The first is the addition of a white-noise force generator for each component of the mechanical resistance. The second is the distribution of the equipartition noise power according to the frequency response of the sensor. And, the third is the application of a software electronic-circuit simulator to the mechanical equivalent circuit of a device. Gabrielson's work also discussed the complementary relationship of shot noise (nonequilibrium) and thermal noise (equilibrium).

The second study was performed at NASA Langley. The researchers measured noise from air condenser, piezoresistive, electret condenser and ceramic microphones (Zuckerwar *et al* 2003). Theoretical models of the respective noise sources within each microphone were developed, and then used to derive analytical expressions for the total noise power spectral densities. Several additional noise sources for the piezoresistive and electret microphones were modeled, and found to contribute significantly to the total noise. Experimental background noise measurements were taken using an upgraded acoustic isolation vessel and the data acquisition system. Those results were compared to the derived models. The models were found to yield power spectral densities consistent with the experimental results. The findings showed that the $1/f$ noise coefficient is strongly correlated with the diaphragm damping resistance, irrespective of the detection technology, i.e. air condenser or piezoresistive.

In the third research project, researchers from Knowles Electronics made noise measurements on their MEMS

miniature electret microphone, typically used in hearing aids (Thompson *et al* 2002). A circuit model was developed from the measured data to determine the noise sources within the microphone. The dominant noise source depends on the frequency range. Electrical noise from the amplifier circuit that buffers the electrical signal from the microphone diaphragm is dominant above 9–40 Hz. Thermal noise originating in the acoustic flow resistance of the small hole present in the diaphragm to equalize barometric pressure dominates after that up to 1 kHz. Between 1 kHz and 9 kHz, the primary noise originates from the acoustic flow resistances of sound entering the microphone and propagating to the diaphragm.

The fourth study was on the characterization and noise analysis of capacitive MEMS acoustic emission transducers. Acoustic emission as an ultrasonic wave is generated when elastic energy is released in a structure by permanent and irreversible change. It is widely used to detect and locate faults in the structure. Resonant-type capacitive MEMS transducers were developed at Carnegie Melon University for the above purpose. Wu *et al* (2007) reported the noise analysis and gave a discussion of noise sources of device. Their analysis identified Brownian noise, caused by collisions between the air molecules and suspended diaphragm, as the dominant source. Furthermore, they observed that the noise is independent of the quality factor (Q) of the transducer.

Q3 The work conducted at the University of Florida investigated the excess noise in a silicon piezoresisitve microphone (Dieme *et al* 2006). This group measured the noise power spectra for both commercial and research-prototype MEMS piezoresistive microphones as a function of applied voltage bias for both free and blocked membranes. They found evidence that the fundamental noise sources are divided into frequency-independent thermal noise and frequency-dependent $1/f$ excess noise, where the latter dominates at low frequencies. They also found a bias dependence and membrane independence of the output noise, indicating that the primary source of the excess noise is electrical in origin.

Beside these five noise studies, many MEMS microphone designers investigated the noise sources of their products. The design and fabrication of a low-voltage, low-noise differential silicon microphone was described (Rombach 2002). The microphone was designed with two back-plates for two advantages. Firstly, the microphone could offer twice the signal of a single back-plate microphone due to the symmetrical arrangement of the two back-plates. Secondly, the bias field was 30% higher compared to a single back-plate microphone, resulting in higher sensitivity and wider linear dynamic range. The noise performance was measured using a low-noise amplifier and an FFT analyzer. It was observed that at lower frequencies, the spectrum was dominated by the ambient acoustical noise up to a few kHz. Further investigation would be required to find the source of the white noise that caused the offset in the noise spectrum. This work indicated that the white noise might have originated from a higher serial resistance of the silicon back-plates and membrane.

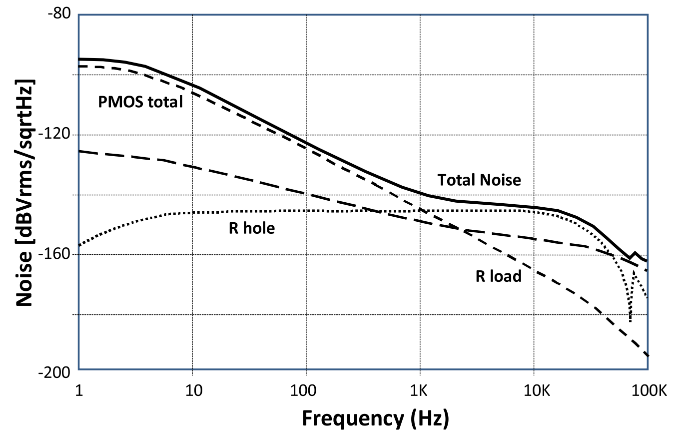

Figure 8. Plot of the contribution of individual noise sources for a silicon microphone (Brauer *et al* 2004).

Another study developed a general SPICE-based model of a silicon microphone system (Brauer *et al* 2004). The acoustical and mechanical, as well as electrical behaviors of the microphone were considered in developing the SPICE model. The model also took into consideration the effect of individual noise sources and their contributions to the total noise. Several experiments were performed to obtain the key parameters to develop the model. The measurements for sensitivity and noise characteristics were performed in a pressure chamber. In that experiment, the dimensions of the chamber were small enough to prevent the reflections of acoustic waves; hence, the pressure was constant at any position. The noise was measured in the same chamber, but with a greater accuracy because of grounding to prevent electromagnetic influence.

Further analysis indicated the effects of individual noise sources on the silicon microphone. Figure 8 shows the amplitude of the noise sources as a function of frequency. It is observed that two noise sources dominate, namely the load resistance, R_{load}, which injects electrical charges into the membrane, and the acoustical resistance, R_{hole}, the resistance through the perforated back-plate. Q4

Another work characterized a piezoresistive silicon microphone designed for aeroacoustic measurements (Arnold *et al* 2001). These devices were characterized in terms of linearity, frequency response, drift, noise and power. Measurements of the noise power spectral densities for eight microphones, biased at 3 V, were performed in a Faraday cage. Figure 9 shows a plot of the noise measured with a DUT versus the system noise. The $1/f$ noise intersects with the thermal noise at approximately 10 kHz for the DUT. The hump in the data between 1 and 10 kHz is believed to be the result of a trap mechanism. The spikes in the data are from deterministic interference at harmonics of 60 Hz and 20 kHz. Since the signals are present in both measurements, their effect can be negated by subtraction of total power at each frequency.

In addition to the above noise studies on silicon microphones, several designers (Ko *et al* 2002, Neumann and Gabriel 2001, Scheeper *et al* 2003) use the noise theories to enhance the sensitivities of their devices.

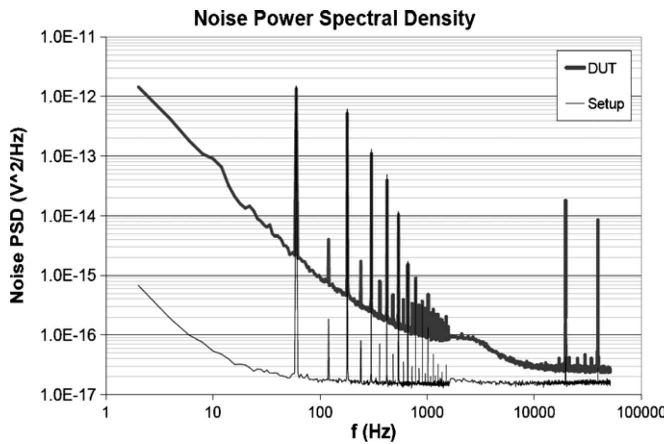

Figure 9. Noise PSD of a piezoresistive silicon microphone (Arnold *et al* 2001).

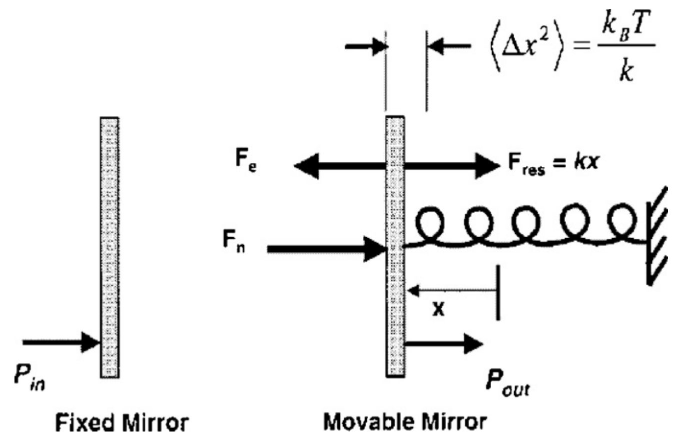

Figure 10. Physical model of optical cavity with thermal noise force (F_N) included (Tucker *et al* 2002).

12. Optical MEMS

Thermal noise is the dominant noise source in optical MEMS. This is due to the fact that thermal energy induces motion in opto-mechanical devices. This type of noise limits the spectral resolution in optical cavities or the sensitivity of the cantilever mass detectors with optical readouts (as discussed in section 7). One paper surveyed some of the most common thermal effects in micro-mechanical optics (Talghader 2004). It reviewed the fundamental heat transfer mechanisms of conduction, convection and radiation, in regard to typical micromirror structures. A simple measurement technique to extract thermal conductance was described. The interface thermal conductance was discussed using recent experimental data on actuated micro-mechanical structures and squeezed-film theory. The paper also explained deformation due to thermal expansion in terms of an analytical elastic model.

Another work by Tucker *et al* (2002) examined the thermal noise and radiation pressure effects in MEMS Fabry–Perot tunable filters and lasers. Both applications require cavities with extremely high mechanical stability. Small perturbations in mirror motion caused by thermal noise degrade the spectral resolution. The Fabry–Perot optical cavity model is shown in figure 10.

The cavity consisted of a fixed mirror and a movable mirror. In the movable mirror, the fluctuations in mechanical energy along the optical axis were set equal to the average thermal energy in each degree of freedom. The mean squared deviation in the position of the mirror $<\Delta x^2>$ is indicated in figure 10. The model showed that the change in mirror position caused a change in the cavity length, and therefore a change in the cavity resonance. The work also examined the frequency response of the thermal-mechanical noise. The mirror position was expected to fluctuate on the time scale of the order of, or longer than, the mechanical response time. But the amplitude of fluctuations should fall off rapidly at frequencies higher than the inverse of that time. A small signal analysis using a force equation for mirror position and voltage showed that the frequency response of the resonance was that of a standard second-order low-pass filter.

Another study (Supino and Talghader 2002) analyzed the thermal properties of a tip-tilt micromirror for the operation in air and vacuum. The studies of noise sources associated with tip-tilt micromirrors were performed analytically and experimentally. This work concluded that three noise mechanisms were present in micromirrors, namely Johnson noise, $1/f$ noise and thermal conductance noise. The first two were standard noise mechanisms that were present in all resistor-type devices. Thermal conductance noise became significant if the device had a small thermal mass.

Two works from University of Berkeley (Zhao *et al* 2002, Choi *et al* 2004) designed, fabricated and tested an optomechanical uncooled infrared imaging system. Detailed noise analysis was performed to find the noise-equivalent temperature difference (NETD) of this system, which was determined from the system's total noise level. All noise sources were analyzed to compute the total noise. The first source was thermodynamic fluctuation noise. This noise source exists in a thermodynamic system that exhibits random fluctuations in temperature, based on the statistical nature of the heat exchange with the environment. The second was temperature fluctuations caused by temperature instabilities on the substrate. The third noise source was vibration noise that originated from thermal and external sources. The last noise source was the optical readout noise, both from CCD and the laser. Figure 11 shows the total noise spectrum of the light intensity from the vertical cavity surface laser operating at 800 nm.

In addition to these papers, several works covered the effects of noise on the performance of optical systems. The effect of quantum noise on an optical sensor for a gyroscope system was presented (Armenise *et al* 2001). One group analyzed the noise factor in an optical passive ring resonator gyro (Suzuki *et al* 2000). Another paper discussed noise effects on a Hadamard-transform spectrometer (Diehl *et al* 1999). In the latest design of tunable vertical cavity surface emitting lasers (VCSELs), the MEMS mirror used wavelength feedback systems to reduce the Brownian motion that broadens the spectral width of the laser emission (Huber *et al* 2004).

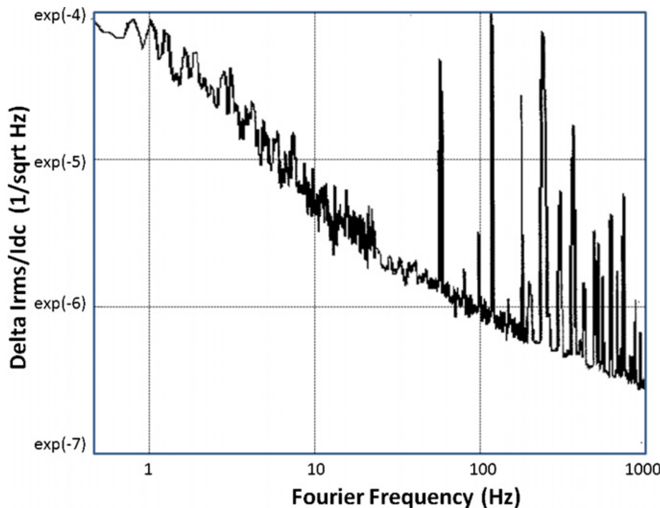

Figure 11. Noise spectrum of the light from a vertical cavity surface laser. The relative noise ($\Delta I/I$) over 30 Hz BW is dominated by low-frequency noise (Zhao *et al* 2002).

13. RF MEMS

RF MEMS cover a large range of devices from simple inductors and filters to complex systems such as voltage-control oscillators (VCO). MEMS RF switches are available commercially. Many studies of the noise characteristics of RF MEMS are available. In general, the phase noise is the dominant noise source for RF MEMS. This section highlights noise research on MEMS RF devices, including an inductor, switches and a switch-based phase shifter, resonator, voltage control oscillator and resonator oscillator.

The first paper reported the noise associated with mechanical deformation of a MEMS inductor (Dahlmann and Yeatman 2002). The device was fabricated in a fully parallel surface micromachining process. One concern about this fabrication approach was that the suspended inductor or the membrane supporting the inductor was susceptible to mechanical loading. Therefore, this study attempted to estimate the variation of the electrical characteristics and the associated noise that was due to the physical deformation of the structure. The geometric model was developed based on the fabricated inductor. The estimation of the noise due to mechanical deformation was carried out in three steps. First, the deformation was calculated numerically as a function of the mechanical loading. Second, the change in inductance was calculated numerically as a function of displacement. Computer programs were used to perform the calculations in both steps. Finally, the noise power due to amplitude and phase variation of the RF signal was calculated analytically. From the data obtained, it was concluded that the amplitude of the signal noise could be equal to or greater than the thermal noise depending on three factors, namely the bandwidth of the system, the signal amplitude and the mechanical loading.

A second paper analyzed the effects of Brownian noise, acceleration, acoustic and power supply noise on a switch-based phase shifter (delay) circuit (Rebeiz 2002b). The analysis was performed for capacitive-shunt MEMS switches and metal-to-metal contact series MEMS switches. Several interesting observations about phase noise were made. First, a well-designed MEMS shunt switch possesses a negligible phase noise from thermal mechanical effects (Brownian noise). The phase noise was found to be so low that it was hard to measure using even the best phase noise measurement equipment. However, it was also observed that low-resistance shunt switches, and switches that were suspended at low gap heights, gave 20–40 dB higher phase noise. Second, varactor-based phase shifters had a relatively high phase noise due to the capacitances used in the design. Third, distributed phase shifters had phase noise that was around 20 dB lower than the varactor-based design, but still 20 dB higher than switched network designs. Fourth, the series switches had virtually no phase noise in the reflect mode, since their up-state capacitance was extremely low. This work also concluded that the contributions of acceleration, acoustic and bias voltage noise on MEMS phase shifters and switches were quite low for an acceleration noise of 10 g or less, an acoustic sound pressure level (SPL) of 74 dB or less and a voltage bias noise of 0.3 V or less, respectively. A similar approach in the subsequent work was used to analyze noise of RF MEMS switches, varactors and tunable filters (Dussopt and Rebeiz 2004). The latest work by Kaajakari *et al* (2005) analyzed phase noise in capacitively coupled microresonator-based oscillators. A detailed analysis of noise mixing mechanisms in the resonator was presented. Capacitive transduction was shown to be the dominant mechanism for low-frequency $1/f$-noise mixing into the carrier sidebands.

In another work, static phase noise and vibration sensitivity of a thin-film resonator (TFR) filter operated at 640 and 2110 MHz were measured (Birdsall *et al* 2002). The evaluation of the TFR filter's short-term frequency stability and vibration sensitivity was accomplished by installing the filter under test as the frequency control element in an oscillator with a low loop delay. A 50 Ω amplifier was used in the setup as the oscillator sustaining stage. The results of the experiment showed that the short-term frequency instabilities of the TFR filters were small compared to those induced in the oscillator signal by the sustaining 50 Ω amplifier phase modulated (PM) noise.

A fourth study involved accurate simulation of phase noise in MEMS voltage control oscillator (VCO) circuits (Behera *et al* 2005). This work employed the numerical solution of device level equations to compute the capacitance of a MEMS capacitor. The phase noise was then determined by combining the computed noise from the MEMS capacitor with a nonlinear circuit-level noise analysis. To ensure an accurate simulation, this capacitor model took into consideration the effects of three noise sources: oscillator phase noise, which consisted of electrical thermal noise, $1/f$ noise and mechanical–thermal vibration noise. After the completion of the capacitor model, the circuitry for the MEMS VCO was used to perform the nonlinear noise analysis. An 800 MHz single-ended Colpitts VCO implemented in HP 0.8 μm CMOS technology was chosen for this purpose. Figure 12 shows the simulated noise spectrum of the modified MEMS VCO. The offset frequency is referenced to the mechanical resonant frequency. The contributions of individual noise sources are shown in the

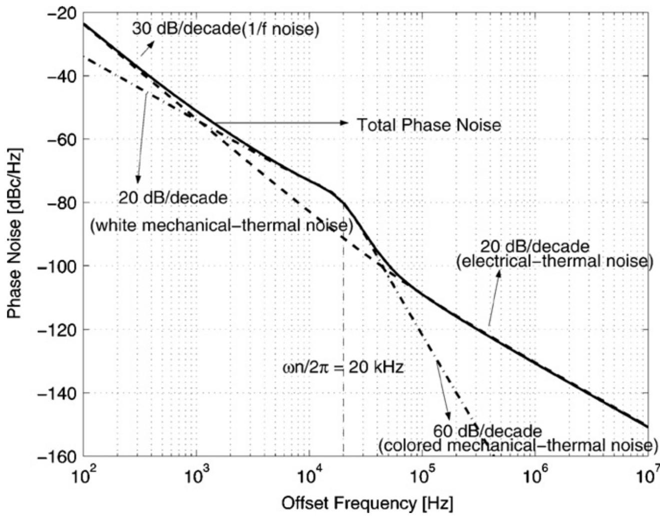

Figure 12. Simulated noise spectrum of a MEMS voltage controlled oscillator (Behera *et al* 2005).

Table 2. Values of Q_m at three different frequencies (Behera *et al* 2005).

Offset frequency	Measured ($Q_M = 15$)	Simulated ($Q_M = 15$)	Simulated ($Q_M = 5$)	Simulated ($Q_M = 1$)
10 kHz	−81	−80.4	−77.6	−73.1
100 kHz	−110	−109.1	−109.1	−108.9
3 MHz	−139	−140.8	−140.8	140.8

figure. It was observed that, at low offset frequency, the $1/f$ noise dominated and, the phase noise showed a 30 dB per decade fall. The electrical-thermal noise dominated for frequencies higher than the mechanical resonant frequency of 20 kHz, where the phase noise showed a 20 dB per decade decay.

The simulated values of the total phase noise for different values of quality factors, Q_m, were calculated in the second part of the work. The results showed that an improvement in phase noise could be seen for increasing Q_m at low offset frequencies. However, as the offset frequency became greater, the dependence of the phase noise on Q_m was reduced. Table 2 shows the values of different Q_m at three different frequencies, 10 kHz, 100 kHz and 3 MHz.

Similar work to simulate and model the noise of MEMS varactor-based RF VCOs was performed by Sankaranarayanan and Mayaram (2007). The mechanical noise exhibited by the MEMS varactor was presented. It originates from Brownian motion. The Brownian motion transforms to a noise current. A noise current model is therefore used to describe the up-conversion mechanism, which was translated to phase noise.

Another work showed the influence of an automatic level control (ALC) circuit on an oscillator phase noise of a MEMS resonator (Lee and Nguyen, 2003). The 10 MHz MEMS-based resonator oscillator was used as the device under test. This custom-designed system allowed the series oscillator to be controlled by two external ALC circuits. The first circuit controlled the resonator's dc bias, called Vp-ALC. The second circuit controlled the sustaining amplifier gain, called A_v-ALC. The results of the measurement with and without ALC

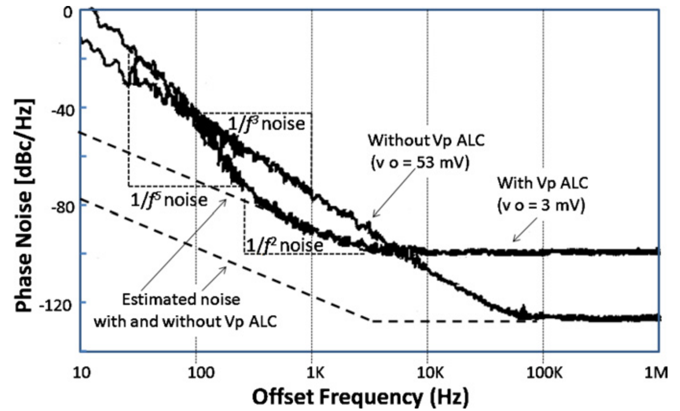

Figure 13. Measurement results for a MEMS resonator (Lee and Nguyen 2003). The acronyms are defined in the text.

engaged are given in figure 13. The results showed that MEMS resonator oscillator exhibited $1/f^3$ phase noise component without the ALC, $1/f^5$ phase noise component when Vp-ALC was engaged and $1/f^2$ phase noise components when A_V-ALC was engaged. The work further investigated the origin of the noise components. It was found that the noise components originated primarily from the nonlinearity in the voltage-to-force capacitive transducer, either through direct aliasing of amplifier $1/f$ noise or through instabilities introduced by spring softening phenomena. The group investigated the noise characteristics of other resonator designs (Nguyen and Howe 1994, 1999, Jing *et al* 2004).

Noise studies of resonators seemed to attract the interest of many groups. One of the studies was performed in Columbia University (Dec and Suyama 2000) and another by Stanford researchers (Agarwal *et al* 2006). It is worth noting that the latest studies of noise in resonators involve nano-scale devices (Vig and Kim 1999, Tamayo 2005, Cleland and Rourkes 2002).

14. SAW devices

The notable work on noise of a SAW device was performed by Enguang (2002). He conducted theoretical and experimental studies of surface-related phase noise of surface acoustic wave (SAW) resonators. The surface phase noise was viewed as a stochastic process resulting from particle molecular adsorption and desorption processes on the device surface. SAW devices have the specific property of extremely high surface sensitivity. They are very prone to be perturbed by mass loading of gas molecules, which this work predicted was the possible source of the noise characteristics. Based on the data, it was found that some volatile vapors, which interacted with the SAW resonator, were able to change the resonator's noise characteristics. These changes were generated by variations in the rate of adsorption and desorption of the surface particles. This work also predicted that the surface molecular motion noise might exist in other electronic devices as the dimensions shrink.

The next two works employed SAW devices as chemical sensors. McGill *et al* (1998) compared the performance of SAW chemical sensors that used a variety of coating

Table 3. Calculated oscillator phase noise performance and spectral densities of frequency fluctuations using measured residual phase noise data of SAW devices with various deposition techniques (McGill *et al* 1998).

Device	Flicker coefficient (rad $Hz^{-1})^2$	Deposition technique	Residual noise floor (dBc Hz^{-1})	Loaded Q	L_{osc} (1) (dBc Hz^{-1})	$S_{\delta f}(1)$ (Hz^2 Hz^{-1})
1	4.0×10^{-38}	Uncoated	−160	7922	−38	0.16×10^{-3}
2	5.14×10^{-38}	Uncoated	−160	7012	−37	0.2×10^{-3}
3	1.2×10^{-34}	Aerosol	−160	3244	−4.0	0.4
4	5.3×10^{-37}	Aerosol	−160	5486	−27.5	1.78×10^{-3}
5	2.3×10^{-36}	MAPLE	−160[a]	6747	−21.5	7×10^{-3}
6	7.22×10^{-37}	MAPLE	−160[a]	7440	−26	2.5×10^{-3}
7	1.6×10^{-36}	MAPLE[b]	−160[a]	5643	−21	8×10^{-3}

[a] Estimated value.
[b] Mulitple resonance modes observed, amplifier flicker noise coeff = 5.02×10^{-14}.

materials and deposition techniques. Residual phase noise measurements were made as one of the performance parameters. The noise measurements were performed on SAW sensors with and without polymer coatings. The residual phase noise at 1 Hz, the white noise floor, the power law dependence on the offset frequency and the $1/f$ corner were measured. This work predicted the system performance of the oscillator-based SAW sensors based on measured data and the modified Leeson's noise model of the loop oscillator, as shown in table 3.

They concluded that the polymer spray-coated SAW devices exhibited large variation of the loaded quality factor (Q) and residual phase noise. In some cases, additional $1/f^2$ noise dependences existed when the frequency of the phase noise exceeded the bandwidth of the resonator. Furthermore, there was no obvious correlation between loaded Q and the phase noise.

15. Flow sensors

Flow sensors are one of the emerging MEMS products. Because they are still in development stage, few works were found on the noise studies for flow sensors. In one project (Radhakrishnan and Lal 2002, 2003), the Cornell researchers presented a scalable microchannel-embedded cantilever flow sensor with electronic readout. The scalable nature of the sensor addressed the need to employ arrays of flow sensors to characterize localized flow patterns. The electronic readout addressed the need to integrate flow sensors in micro-fluidic channels for closed-loop flow control. The group also presented a prediction of the noise characteristics for flow measurements, based on the results obtained using prototype flow sensors. It was observed that the electrical-thermal noise was the main noise source. This thermal noise originated from the resistors used in a Wheatstone bridge in the interface circuitry of the flow sensor. Figure 14 presents the results of the noise analysis. The data showed that the noise came from two sources: the amplifier and the flow sensor. The experimental results also showed that the flow in the channel caused thermal gradients along the channel, which affected the performance of the device considerably. This work suggested the use of nickel cantilever beams to shunt away any thermal fluctuations that existed in the channel. This improvement would

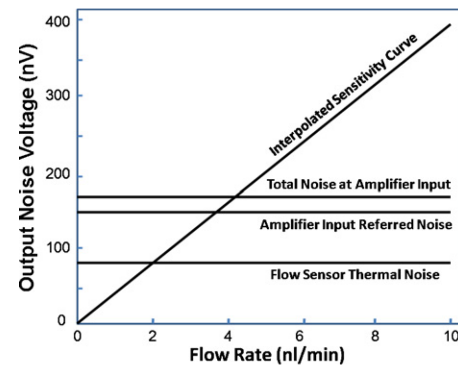

Figure 14. Flow sensor output voltage and noise from the amplifier and flow sensor (Radhakrishnan and Lal 2003)

make the device more immune to flow-induced temperature changes.

We also found another study that injected white noise into the circuits of the micro-fluidic flow sensor (Law and Afromowitz 2000). This was deliberately done to characterize the performance of the sensor with and without the white noise source. Besides these works, there are several reports of noise analyses to determine the limit of sensitivity of particular flow sensor designs (Yoon and Wise 1992, Wu *et al* 2000, Kaltsas and Nassiopoulou 1999).

16. Chemical sensors

Miniaturization is the recent trend in analytical chemistry and life sciences. The applications cover a broad range, including micro arrays, DNA sequencing, sample preparation devices, and cell separation and detection functions, as well as environment monitoring with gas sensors (Nguyen and Wu 2005). **Q5** The number of archival journal papers in this area has increased drastically over the past few years. We first review several papers on noise in chemical sensors. The next section will be on noise in bio-MEMS.

One of the notable studies was performed Hoel *et al* (2002), where the conduction noise measurements were carried out for Au films covered by a thin layer of tungsten trioxide (WO_3) nanoparticles, within 0.3–45 Hz frequency range. An 'invasion noise model' was developed based on the data collected from the experiment. This model was founded

on the idea that the noise was related to the insertion and extraction of mobile chemical species, in this case onto and from the WO_3 nanoparticles. The results show that exposing the Au and WO_3 films to alcohol vapor will gradually increase the noise intensity, which went to a maximum after 15 min.

Another study used the noise characteristics to improve the selectivity of semiconductor sensors (Shaposhnik *et al* 2005). The total noise PSD of the sensors are composed of both chemisorption of gases and vapors, and chemical reactions between reducing gases and air oxygen that occur on the sensor surface. A gas sensors designed for odor recognition of a complex sample could be realized by combining the electric resistance and its noise characteristics. Similar work was performed by Kish *et al* (2000), whereby the electronic noses and tongues utilized the conduction noise data, taken at the output of a chemical sensor. It is shown that one single sensor may be sufficient for realizing an electronic nose or tongue for several analytes.

Several groups developed noise models of chemical sensors. Gomri *et al* (2005) proposed a theoretical description of adsorption–desorption noise in metal oxide gas sensors using Langmuir and Wolkentein models. They found that the adsorption–desorption noise (A–D noise) part of the total noise spectra has a Lorentzian distribution, and applied the proposed model for simulating the oxygen chemisorption-induced noise of the metallic-oxide gas sensors. Another work from the Stanford researchers proposed a general circuit model for the electrical noise of electrode–electrolyte systems, intended for electrochemical sensors (Hassibi *et al* 2004). In their approach, the analytical model of all the noise sources that contributed to the overall noise PSD of the system was calculated. They showed that the current and voltage fluctuations originated from either thermal equilibrium noise created by conductors, or nonequilibrium excess noise caused by charge transfer processes produced by electrochemical interactions. The presented electrical noise model could be used to explain thermal noise in sensing electrodes, shot noise in electrochemical batteries and $1/f$ noise in corrosive interfaces. In addition to these works, there are many chemical sensor designers who performed noise analysis on their devices, such as in Vidybida *et al* (2005), Wang *et al* (2005) and Fadel *et al* (2004) for the purpose of increasing the sensitivities of their prototypes.

17. Biosensors

The same Stanford group, which proposed the electrical noise model of electro-chemical sensors, published another work to estimate the sensor inherent noise PSD of an affinity-based DNA sensor (Hassibi *et al* 2005). This project involved determining the statistical behavior of affinity-based biosensors. The noise originated from the probabilistic molecular-level bindings within the sensing regions, as well as the stochastic mass-transfer processes within the reaction chamber. They modeled the dynamic behaviors of the sensor by a Markov process, by extracting the Markov parameters from the reaction kinetic rates, diffusion coefficients and reaction chamber boundary condition. Similar to Gomri *et al* (2005), they predicted a Lorentzian profile for the fluctuation PSD.

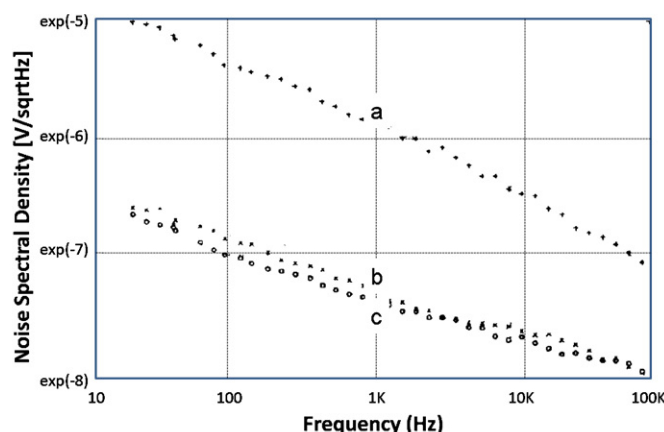

Figure 15. Noise from an integrated four-electrode structure: (*a*) outer (current) electrodes, (*b*) inner (voltage) electrodes with current and (*c*) inner electrodes without current (Kordas *et al* 1994).

Another work attempted to characterize the properties of integrated micro-electrodes for a (CMOS) compatible medical sensor (Kordas *et al* 1994). The thermal and excess noise of the integrated electrodes was measured, similar to the approach of Radhakrishnan and Lal (2003). Figure 15 shows the noise characteristics of the micro-electrodes. The data obtained from the measurements revealed several facts. First, the thermal noise showed a frequency behavior following the impedance characteristics of the electrodes. Second, excess noise due to measuring current was much higher than without current, and it also showed frequency dependence. Third, the sensor performance was only affected by a small amount of thermal noise. Finally, the excess noise did not occur at the sensing electrodes.

Numerous studies were performed in the past few years for the fabrication of DNA array chips. One of these (Li *et al* 2003) explored the need for a pre-hybridization step for DNA detection to reduce background noise. Pre-hybridization is a process where random DNA fragments are applied to coat the chip surface after the probe attachment. This step is done to reduce the background signal caused by nonspecific absorption of target DNA and gold nanoparticles onto the entire surface of the chip. The results showed that the current level from the cell with DNA hybridization was almost equal without and with pre-hybridization, but the current due to background absorption was significantly reduced after a pre-hybridization step. This work showed that the pre-hybridization step increased the SNR of the chip and reduced the absorption noise. Similar work was reported in Tu *et al* (2002).

In addition to these works, there were other studies that examined the noise characteristics of biosensor designs, namely those by Hagleitner *et al* (2002), Kim *et al* (2001), Gupta *et al* (2004), Savran *et al* (2002, 2003) and Berney *et al* (2000). In general, two noise sources account for the limited performance of biosensors. The first one is the absorption and desorption noise and the second source is electrical thermal noise.

18. Data storage devices

MEMS are expected to have a bright future for information storage devices. A new technique, which is called 'nano-cuneiform', is being explored by some companies for this purpose. In this case, MEMS enable a new type of storage technology. In addition, MEMS actuators are also being considered for conventional magnetic drives to give finer control of the read–write heads, which in turn decreases the track spacing and increases storage density. In this application, they can be part of magnetic disc systems, extending their capabilities to higher densities. We review both possibilities.

The new intrinsically MEMS storage technology is called the 'millipede' by IBM, its developer (Eleftheriou *et al* 2003). Electrostatic actuation is used to actively control the height with respect to the data storage media of each probe tip in a 32 by 32 array of AFM tips. Heat deforms the media to provide a stored bit. Capacitive sensing is used to read out bits from the media. The noise of the Millipede system is composed of largely Johnson noise from the sensor and the reference cantilever resistances, which reach a temperature of 350 °C during the read operation, and from the low-pass filter resistances, as well as noise from the operational amplifiers. The SNR at the detection point due to these noise sources is typically in the range of 16–20 dB.

Hitachi researchers presented a fast noise analysis of thermal fluctuation noise on micromachined magnetoresistive devices (van Peppen and Klaassen 2006). Normally, noise analyses by micromagnetic simulations are computationally very intensive and require enormous amounts of simulation time. This paper presents a faster micromagnetic method to arrive at the noise and small signal dynamics of these devices. It showed the effect of spin torque transfer on the noise and on the small signal dynamics of a current perpendicular to a planar giant magnetoresistive (GMR) sensor. Further work was performed on magnetic simulation of noise, SNR, and bandwidth for the most common types of magnetic head: tunneling magnetoresistive heads and GMR heads (Klaassen *et al* 2006).

Carnegie Mellon U researchers presented a standard system design consideration for magnetic storage devices that employed MEMS devices for positioning of a magnetic probe device over a magnetic media (Carley *et al* 2001). In this design, the electrostatic actuation and capacitive sensing were used to actively control the height of each probe tip, with respect to the media. It was found that the position sensing circuit generated noise. This in turn limited the SNR with which the Z separation between the media and the probe tip could be controlled. Investigation revealed that the dominant electronic noise source for the positive sense circuit was the thermal noise of the MOS amplifier. In addition, there were two other non-electronic noise sources in the system. The first was the thermal vibration of air molecules and of the molecules that make up the MEMS beams, namely the Brownian noise. The second source, also significant, was media noise, as is normally found in magnetic hard disk drives.

A sensitivity study for 40 Gb in^{-2} magnetic recording systems on the fluctuations of head-disk spacing was

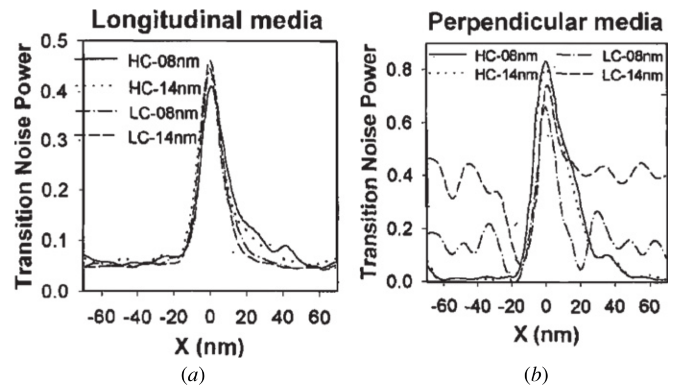

Figure 16. Relative noise power for transitions between bits in two types of magnetic recording media for low (LC) and high (HC) currents and head-disk spacings of 8 and 14 nm. The horizontal axis is the distance along the recording direction (Yuan *et al* 1999).

reported by Yuan *et al* (1999). The micromagnetic simulation was carried out to obtain the behaviors of two noise sources, transition noise and cross track noise. The simulation considered two magnetic configurations of recording systems, conventional longitudinal recording and single layer perpendicular recording. The first part of the work was to compute the transition noise. The results showed that in the longitudinal recording media, there were no big differences among the transition noises. However, higher writing current and lower spacing caused the transition noise to have a somewhat lower peak value. The simulations using single layer perpendicular recording showed that the transition noise was not sensitive to the spacing fluctuation when high writing current was applied. The computations further showed that, when a lower writing current was applied, higher spacings had larger transition noise, and the noise between the transitions increased drastically as the spacing changed from 8 nm to 14 nm. Figure 16 shows the transition noise profiles for both magnetic configurations. The second part of the work attempted to characterize the cross track noise for two magnetic configurations. The results of the simulations show that higher writing current consistently produced bigger track edge noise. Furthermore, both media were very sensitive to the spacing fluctuations. The lower spacing produced more cross track noise. However, single layer perpendicular media with lower current writing generated more on-track noise as the spacing was wider. This work proved that current selections were crucial in reducing the noise sources in both types of media.

There were other works that should be briefly mentioned. One such work (El-Sayed and Carley 2002) attempted to identify the noise sources on a 100 Gb in^{-2} magnetic-force-microscopy MEMS-actuated mass storage device, with a follow-up paper 3 years later (El-Sayed and Carley 2005). Chen *et al* (2001) and Igarashi *et al* (2003) attempted to find the causes of instabilities in magneto-resistive recording heads, and Pannetier *et al* (2005) investigated noise of GMR sensors. Q6

19. Magnetic MEMS

MEMS-based magnetic sensors are used for a wide range of applications. Some of the designers performed noise studies on their magnetic sensors. One group developed a magnetic-field sensor that is based on an electron tunneling transducer (DiLella *et al* 2000). The noise analysis was performed, and it was found that the dominant source of the observed noise in the device was low-frequency air pressure fluctuations.

There is also one noise study on another type of magnetic sensor, called miniature fluxgate magnetometers (Dimitropoulos 2005a, 2005b). Several noise sources of different origins have been found, namely (a) the magnetic (Barkhausen) noise, (b) the noise superimposed to the excitation waveform, (c) the noise generated due to electromagnetic interference and (d) the noise generated due to mechanical vibration of fluxgate cores. The various noise sources have been modeled and their power spectral density estimated from the experimental results. Similar work was performed by Joisten *et al* (2004). The latest study reported the dc and ac magnetic field dependence of the low-frequency noise in a MEMS flux concentrator device containing a giant magnetoresistance spin valve (Ozbay *et al* 2006, Edelstein *et al* 2006).

20. Conclusion

We pointed out the fundamental aspects of the different kinds of noise mechanisms. Some experimental works have found either electrical or non-electrical noise to be dominant. It is critical for designers of MEMS, which will be used for low-signal applications, to know the dominant noise mechanisms in order to produce devices that will have lower noise from those mechanisms.

We found that there are substantial works on noise in MEMS, particularly in the area of modeling and measurements of inertial MEMS and RF MEMS. The growing numbers of noise studies in the area of optical, chemical and bio-MEMS are noteworthy, as is the dearth of noise studies of MEMS pressure sensors.

Different types of MEMS were found to have interesting noise characteristics. For example, RF MEMS, especially high-frequency resonators, are more susceptible to mechanical noise than other classes of MEMS. While most of the effects of noise on MEMS are undesirable, noise is exploited by improved sensing in some chemical sensors. It seems possible that the use of noise to determine the degradation of MEMS over time and use will prove fruitful.

One of the attractive features of noise studies in MEMS is the fact that the small sizes and masses of their parts can bring both intrinsic electrical and non-electrical mechanisms into play. Hence, there appears to be a need for theoretical and experimental work on their interactions. Such research should be more important for sensors and actuators with very small, nano-scale components.

There is clearly much room for additional experimental studies of noise in all types of MEMS. The same is true of theoretical and computational studies. The equations, algorithms, techniques and computers are all available for such works. Both Monte Carlo and molecular dynamic computations should prove interesting and, possibly, useful for the study of noise in MEMS, including the interactions of various active mechanisms.

It is our hope that this review will provide a useful basis for further research on noise in MEMS, both on fundamentals, and on mechanisms and devices that have not been much studied to date. The topic is as intellectually challenging as it is important for MEMS employed in low-signal applications.

Acknowledgments

Interest in and valuable comments on this work by Dr D S Ong and Bassam Noaman are recalled with pleasure. Supports from Professor HT Chuah and from Professor AR Faidz are also greatly appreciated.

Appendix. Units for noise

Units are utterly necessary in science, engineering and many other fields, such as business (dollars, euros, pounds, etc). They enable quantification of diverse parameters. But, units present two problems. The first challenge is to understand them, both their definitions, plus whatever is part of the definitions. For example, energy can be expressed as joules, which are defined as the amount of energy expended when a force of 1 N is applied over a distance of 1 m. The second problem is conversion of units. Energy can be expressed by any of several units, including electron volts, calories, ergs, BTUs or quads. The numerical factors needed to convert from one unit to another are diverse, but are readily available on the Internet. Both of the general problems with units apply to the units used to quantify various types of noise, which are commonly frequency dependent.

The units used to express noise levels are independent of the mechanisms, which generate the noise. Of the many units used to describe noise, probably the most physical and understandable is noise power. It is frequency dependent, so a graph of noise power as a function of frequency is commonly called the power spectral density (PSD). The magnitude of the PSD is the power within some small bandwidth (BW) expressed in Hz. The absolute value of the PSD depends on the BW, that is, there will be less power in a narrow spectral region (BW) and vice versa.

The absolute value of the noise power can vary widely. Hence, the noise power P is usefully expressed on a logarithmic scale in decibels relative to a level of 1 mW, that is, dBm. The noise power at some frequency for some BW is given by the equation $\text{dBm} = \log_{10}(P/1\text{ mW})$. This is the quantity provided by many commercial spectral analyzers. If the PSD is stationary, that is, if it is unvarying with time, then the product of its value for any frequency interval, and the length of some time interval of interest, gives the noise energy in the particular bandwidth during that time period.

Other reference levels for noise in dB can be found. For example, dB_V are referred to 1 volt. dB_U have a basis of 0.7746 volts. ‘U’ in dB_U has various meanings, including

(a) unloaded source, (b) unspecified load impedance and (c) unterminated.

For electrical noise, a basic relationship is used to describe noise power P, namely $P = V$ x I. The voltage V and current I (in amperes) are related by Ohm's law, $V = I$ x R, where the resistance R is expressed in ohms. Hence, $P = V^2/R$, as usual within some BW in Hz. Because volts are a fundamental unit in electrical engineering, it is common practice to take the square root of the quantity V^2 Hz^{-1} to get 'volts per root Hz'. Multiplicative factors, such as the resistance R, can either be ignored, or assumed to be the common value of 50 Ω. Sometimes, the voltage is taken as the RMS (root mean square) value, rather than the absolute value.

Volts per root Hz has the advantage of volts being very a familiar unit. But, the price for that convenience is having to deal with the square root of the BW. While this is easy to evaluate numerically, when the BW is known, it is very difficult conceptually. It is neither physical nor easy to internalize, when considering noise at different frequencies or in different systems. That is, volts per root Hz does not refer to an actual physical quantity for which a person can develop a feeling for its magnitude. However unsavory is this unit, volts per root Hz is now firmly established in reports on noise in electrical systems. In fact, similar units are employed even when volts are not involved. For example, 'd per root Hz' is used to quantify noise in displacement (d) detection devices that sense the position of a structure or object. Similarly, 'g per root Hz' is employed for noise in accelerometers, where g is the acceleration due to gravity at the surface of the earth. Figure 7 of this review gives an example of such units for MEMS accelerometers.

The output of most MEMS devices is electrical, so that it is common practice to express their noise in power as dBm Hz^{-1} or in volts per root Hz. However, examination of the experimental plots of noise as a function of frequency in the figures of this paper shows that other noise units are employed for MEMS involving electromagnetic energy, either optical or radio frequency.

Micromachined optical sources include light emitting diodes (LEDs), lasers (especially vertical cavity surface emitting lasers, that is, VCSELs) and heated sources of infrared radiation (notably micro-hotplates). The optical beams emitted by these sources carry noise from various mechanisms. MEMS optics include small mirrors and diffraction elements, such as Fresnel lenses and gratings. A few optical detectors qualify as MEMS, that is, they are produced by micromachining processes. Both MEMS optics and detectors can influence the relative intensity noise carried by light in the visible and the nearby ultraviolet and infrared spectral regions, and the signals that result from incidence of these wavelengths on detectors.

The intensity of optical beams varies over time for a variety of reasons, such as thermal instabilities, and pump variations or cavity vibrations within lasers. The noise of optical beams is often expressed as relative intensity noise (RIN). This is the ratio of the noise, that is, the intensity fluctuations, to the average intensity of the beam. RIN tends to be independent of the absolute intensity. It varies with frequency, and is commonly expressed as dB per Hz at a specified frequency. Note that the intensity can be expressed in units of quanta (photons) per second or energy per second (power).

For radiation detectors that operate in the visible and nearby spectral ranges, the noise-equivalent power (NEP) is used to quantify the noise they introduce into a measurement. The NEP is defined as the signal power that gives a signal-to-noise ratio of unity for specific operating conditions. Detectivity is defined as the reciprocal of the NEP. Hence, detectors with low noise have high detectivity values. More elaborate definitions of detectivity are often used. For example D^* (D-star) is the detectivity normalized to the area of a detector and a unit bandwidth.

Many infrared, THz and microwave detectors are bolometers, which work by responding to the temperature rise due to absorption of radiation. In most cases, the temperature of the scene being viewed by such detectors in systems is of interest. Hence, a temperature-based unit is used to quantify a detector or system noise. NETD stands for noise-equivalent temperature difference. It is the change in the equivalent blackbody temperature that gives a change in radiance onto the detector and instrument that will give a signal-to-noise ratio of unity. The NETD is above, but close to the limit of detection for an optical sensor. The difference in scene temperatures equal to the detector noise is called the detector NETD. The similar difference in scene temperature equal to the system noise is the System NETD. The former is specific to the detector and the latter includes system electronic noise. We note in passing that sensors, other than those relying on temperature rises, also have noise equivalents. For example, pressure sensors have noise-equivalent pressures.

Phase noise is important in modern radio-frequency communications and in a wide variety of digital systems. The units used to quantify phase noise are not as widely understood as are the units discussed above for quantifying the noise power from various electrical or optical sources. Phase noise units are critical to describing the performance of RF communication systems, including RF MEMS, and the performance of digital systems, including those that are part of MEMS devices. The phase noise of an oscillator in an RF system is conceptually related to the jitter in the clock in a digital system.

An understanding of phase noise can start with consideration of a sine wave, which has three characteristics: frequency, amplitude and phase. For a pure time-varying sine wave, all of these quantities are constant. However, in reality, they all have some associated noise. Variations in phase produce deviations in the precise times at which the sine wave is zero. These are equivalent to changes in frequency, which is derived from the time between zero-crossings. Hence, in the frequency domain, the spectrum of the wave is no longer a delta function at the basic (carrier or clock) frequency, but has a distribution around the fundamental frequency. This is applicable to the phase variations of a sine wave (expressed in degrees) and to the time jitter in an electrical, optical or RF digital signal (given in seconds), which are related by the equation

$$\text{Jitter (s)} = [\text{Phase Error}(^\circ)]/[360 \times \text{Frequency (Hz)}].$$

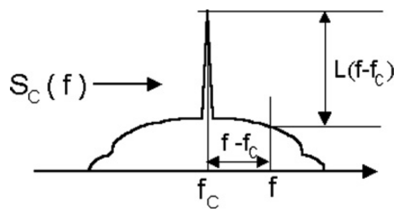

Figure A 1. Drawing of the frequency spectrum due to phase noise on a carrier at $f_{c.}$ (from Wikipedia).

The frequency distribution has a width determined by the magnitude of the phase noise. The frequency-dependent amplitude of the phase noise is determined by the details of the source of phase noise. The schematic in figure A1 shows the PSD, written as $S_C(f)$, for the carrier and the associated distribution due to phase noise. The phase noise spectrum is $L(f - f_c)$, which is referenced to the amplitude of the spectrum at the carrier frequency. The phase noise spectrum is expressed as dBc, that is, decibels relative to the carrier. It is the frequency-dependent power ratio of the phase noise relative to the power of the carrier. The mathematical definition of phase noise is

$$L(f - f_c) = 10\log[S_c(f)/S_c(f_c)] \qquad \text{in dBc.}$$

That is, rather than being referenced to an absolute quantity like milliwatts (for dBm), the phase noise PSD is referenced to the carrier power that exists for a particular situation.

As is usual for a PSD, the magnitude in dBc for phase noise is actually referenced to a particular bandwidth since the absolute value will depend on the BW used to measure the phase noise PSD. That is, the units are actually dBc Hz^{-1}. As with the units discussed above, (power/frequency) has units of (energy/time)/(1/time) or energy.

It must be noted that there are MEMS sources of radio frequencies, specifically oscillators of several types. The units of dBc or dBc Hz^{-1} apply to such oscillators. Further, other MEMS RF devices, such as switches and RF detectors, can increase or otherwise modify the noise in RF signals propagating through them.

The conversion of noise units from one basis to another is sometimes desirable. For example, the power in an optical or RF electromagnetic beam can be expressed equally as the number of quanta (photons) passing per unit of time, or in more common power (energy per time) units.

In summary, the quantitative expression of noise power is generally done relative to an absolute value (commonly 1 mW) for electrical signals, relative to the average power for optical signals, or relative to the power of the carrier for radio-frequency signals. These do not cover all cases, for example, noise in acoustic signals (given as the sound power level), or electrostatic or magnetostatic signals (expressed as field strengths). However, an appreciation of noise units for electrical and electromagnetic signals does cover most of the cases for MEMS and other small devices.

References

Agarwal M *et al* 2006 Effects of mechanical vibrations and bias voltage noise on phase noise of MEMS resonator based oscillators *Proc. 19th IEEE Int. Conf. on Micro Electro Mechanical Systems (Istanbul, Turkey)* pp 154–7

Amini B and Ayazi F 2005 Micro-gravity capacitive silicon-on-insulator accelerometers *J. Micromech. Microeng.* **15** 2113–20

Annovazzi-Lodi V and Merlo S 1999 Mechanical–thermal noise in micromachined gyros *Microelectron. J.* **30** 1227–30

Armenise M N, Passaro V, De Leonardis F and Armenise M 2001 Modeling and design of a novel miniaturized integrated optical sensor for gyroscope systems *J. Lightwave Technol.* **19** 1476–94

Arnold D P, Gururaj S, Bhardwaj S, Nishida T and Sheplak M 2001 A piezoresistive microphone for aerocoustic measurement *Proc. IMECE (New York)* pp 1–8

Bak P 1996 *How Nature Works; The Science of Self-Organized Criticality* (Berlin: Springer)

Behera M, Kratyuk V, Hu Y and Mayaram K 2005 Accurate simulation of RF MEMS VCO performance including phase noise *IEEE J. Microelectromech. Syst.* **14** 313–25

Berney H *et al* 2000 A DNA diagnostic biosensor: development, characterisation and performance *Sensors Actuators* B **68** 100–8

Birdsall S A, Dever P B, Donovan J B, Driscoll M M, Lakin K M and Pham T H 2002 Measurement of static and vibration-induced phase noise in UHF thin-film resonator (TFR) filters *IEEE Trans. Ultrason. Ferroelectr. Freq. Control* **49** 643–8

Boser B E and Howe R T 1996 Surface micromachined accelerometers *IEEE J. Solid-State Circuits* **31** 366–75

Brauer M, Dehe A, Fuldner M and Laur R 2004 Increasing the performance of silicon microphones by the benefit of a complete system simulation *Proc. Int. Conf. MEMS* pp 528–31

Carley L R, Ganger G, Guillou D F and Nagle D 2001 System design considerations for MEMS-actuated magnetic-probe-based mass storage *IEEE Trans. Magn.* **37** 657–62

Chae J, Kulah H and Najafi K 2004 An in-plane high sensitivity, low noise micro-g silicon microaccelerometer with CMOS readout circuitry *IEEE J. Microelectromech. Syst.* **13** 628–35

Chen L, Chen E, Giusti J, Fernandez-de-Castro J and Saunders D 2001 Micro-magnetic and electric analysis on MR head baseline popping and instabilities *IEEE Trans. Magn.* **37** 1343–5

Choi J, Yamaguchi J, Morales S, Horowitz R, Zhao Y and Majumder A 2004 Design and control of thermal stabilizing system for a MEMS optomechanical uncooled infrared imaging camera *Sensors Actuators* A **114** 132–42

Cleland A N and Roukes M L 2002 Noise processes in nanomechanical resonator *J. Appl. Phys.* **92** 2758–69

Dahlmann G W and Yeatman E M 2002 Mechanical noise induced by acceleration or acoustic disturbances in MEMS microwave inductors *High Frequency Postgraduate Student Colloquium* p 10 **Q7**

Dec A and Suyama K 2000 Microwave MEMS-based voltage-controlled oscillators *IEEE Trans. Microw. Theory Tech.* **48** 1943–9

Dec A, Toth L and Suyama K 1998 Noise analysis of a class of oscillators *IEEE Trans. Circuits Syst.* **45** 757–60

Degani O, Seter D J, Socher E, Kaldor S and Nemirovsky Y 1998 Optimal design and noise consideration of micromachined vibrating rate gyroscope with modulated integrative differential optical sensing *J. Microelectromech. Syst.* **7** 329–38

Diehl T, Ehrfeld W, Lacher M and Zetterer T 1999 Electrostatically operated micromirrors for Hadamard transform spectrometer *IEEE J. Sel. Top. Quantum Electron.* **5** 106–10

Dieme R, Bosman G, Nishida T and Sheplak M 2006 Source of excess noise in silicon piezoresistive microphones *J. Acoust. Soc. Am.* **119** 2710–20

DiLella D *et al* 2000 A micromachined magnetic-field sensor based on an electron tunneling displacement transducer *Sensors Actuators* A **86** 8–20

Dimitropoulos P D 2005a Noise sources in miniature fluxgate sensors: Part I. Theoretical treatment *Int. J. Electron.* **92** 499–524

Dimitropoulos P D 2005b Noise sources in miniature flugate sensors: Part II. The case of sensors with Fe77.5Si7.5B15 amorphous wire cores *Int. J. Electron.* **92** 561–82

Djuric Z 2000 Mechanisms of noise source in microelectromechanical systems *J. Microelectron. Reliab.* **40** 919–32

Djuric Z, Jaksic Oand D and Randjelovic D 2002 Adsorption–desorption noise in micromechanical resonant structures *Sensors Actuators* A **96** 244–51

Dussopt L and Rebeiz G M 2004 Intermodulation distortion and power handling in RF MEMS switches, varactors, and tunable filters *IEEE Trans. Microw. Theory Tech.* **51** 1247–56

Edelstein A S *et al* 2006 Progress toward a thousandfold reduction in 1/f noise in magnetic sensors using an ac microelectromechanical system flux concentrator *J. Appl. Phys.* **99** Art. No 08B317

Eleftheriou E *et al* 2003 Millipede-a MEMS-based scanning-probe data-storage system *IEEE Trans. Magn.* **39** 938–45

El-Haks M G 2001 *The MEMS Handbook* (Boca Raton, FL: CRC Press)

El-Sayed R T and Carley L R 2002 Performance analysis of beyond 100 Gb/in/sup 2/ MFM-based MEMS-actuated mass storage devices *IEEE Trans. Magn.* **38** 1892–4

El-Sayed R T and Carley L R 2005 Media and tip trajectory optimization for high-density MFM-based perpendicular recording *IEEE Trans. Magn.* **41** 1209–17

Enguang D 2002 Surface-related phase noise in SAW resonators *IEEE Trans. Ultrason. Ferroelectr. Freq. Control* **49** 649–55

Fadel L *et al* 2004 Signal-to-noise ratio of resonant microcantilever type chemical sensors as a function of resonant frequency and quality factor *Sensors Actuators* B **102** 73–7

Gabrielson T B 1993 Mechanical–thermal noise in micromachined acoustic and vibration sensor *IEEE Trans. Electron. Devices* **40** 903–9

Gabrielson T B 1995 Fundamental noise limits for miniature acoustic and vibration *Sensors J. Vib. Acoust.* **117** 405–10

Gomri S, Seguin J L and Guerin J 2005 Modeling on oxygen chemisorption-induced noise in metallic oxide gas sensors *Sensors Actuators* B **107** 722–9

Gomri S, Seguin J L and Guerin J 2006 Adsorption–desorption noise in gas sensors: modelling using Langmuir and Wolkenstein models for adsorption *Sensors Actuators* B **114** 451–9

Greiner A and Korvink J 1998 Extraction of noise parameters for the macromodelling of MEMS *Proc. Adv. Semiconductor Dev. and Microsystems Conf* pp 311–4

Gupta A, Akin D and Bashir R 2004 Detection of bacterial cells and antibodies using surface micromachined thin silicon cantilever resonators *J. Vac. Sci. Technol.* B **22** 2785–91

Hagleitner C, Lange D, Hierlemann A, Brand O and Baltes H 2002 CMOS single-chip gas detection system comprising capacitive, calorimetric and mass-sensitive microsensors *IEEE J. Solid-State Circuits* **37** 1867–78

Han K H and Cho Y C 2003 Self-balanced navigation-grade capacitive microaccelerometers using branched finger electrodes and their performance for varying sense voltage and pressure *J. Microelectromech. Syst.* **12** 11–20

Hassibi A *et al* 2004 Comprehensive study of noise processes in electrode electrolyte interfaces *J. Appl. Phys.* **96** 1074–82

Hassibi A *et al* 2005 Biological shot-noise and quantum-limited signal-to-noise ratio in affinity-based biosensors *J. Appl. Phys.* **97** Art. No 084701

Hoel A, Ederth J, Kopniczky J, Heszler P, Kish L B, Ollson E and Granqvist C G 2002 Conduction invasion noise in nanoparticles WO_3/Au thin-film devices for gas sensing application *Smart Mater. Struct.* **11** 640–4

Huber D, Corredoura P, Lester S, Robbins V and Kamas L 2004 Reducing Brownian motion in an electrostatically tunable MEMS laser *IEEE J. Microelectromech. Syst.* **13** 732–6

Igarashi M, Hara M, Nakamura A and Sugita Y 2003 Micro-magnetic simulation of magnetic cluster, thermal activation volume, and media noise in perpendicular recording media *Proc. Joint NAPMRC* p 13

Jing W, Ren Z Y and Nguyen C T C 2004 1.156-GHz self-aligned vibrating micromechanical disk resonator *IEEE Trans. Ultrason. Ferroelectr. Freq. Control* **51** 1607–28

Joisten H *et al* 2004 Integrated solutions to decrease micro-fluxgate sensors noise *IEEE Trans. Magn.* **40** 2649–51

Joseph E D, Kar B K, Rohrkemper R and Ger M 1996 Design and noise analysis of an automotive accelerometer *Proc. ISCAS* pp 141–3

Jwang J, Zavracky P M, McGruer N E and Morrison R H 1997 Study of tunneling noise using surface micromachined tunneling tip devices *Proc Int. Conf. on Solid State Sensors and Actuators* pp 467–70

Kaajakari V, Koskinen J K and Mattila T 2005 Phase noise in capacitively coupled micromechanical oscillators *IEEE Trans. Ultrason. Ferroelectr. Freq. Control* **52** 2322–31

Kajita T, Moon U and Temes G C 2002 A two-chip interface for a MEMS accelerometer *IEEE Trans. Instrum. Meas.* **51** 853–8

Kaltsas G and Nassiopoulou A G 1999 Novel C-MOS compatible monolithic silicon gas flow sensor with porous silicon thermal isolation *Sensors Actuators* A **76** 133–8

Kim J, Kim B G, Yoon E and Han C 2001 A new monolithic micro biosensor for blood analysis *Proc. IEEE Int. Conf. MEMS* pp 443–6

Kish L B, Vajtai R and Granqvist C G 2000 Extracting information from noise spectra of chemical sensors: single sensor electronic noses and tongues *Sensors Actuators* B **71** 55–9

Klaassen K B, van Peppen J C L and Xing X Z 2006 Simulation of noise, signal-to-noise and bandwidth of TMR and CIP/CPP GMR heads *IEEE Trans. Magn.* **42** 108–13

Ko S, Kim Y, Lee S, Choi S and Kim S 2002 Piezoelectric membrane acoustic devices *Proc. IEEE Int. Conf. MEMS* pp 296–9

Kordas N, Manoli Y, Mokwa W and Rospert M 1994 The properties of integrated micro-electrodes for CMOS-compatible medical sensors *Proc. 16th Annu. l Int. Conf. IEEE Eng. in Medicine and Biology Soc* pp 828–9

Korvink J G and Greiner A 2002 *Semiconductors for Micro and Nanotechnology* (New York: Wiley)

Kovacs G 1998 *Micromachined Transducers Sourcebook* (New York: McGraw-Hill)

Kulah H, Chae J, Yadzi N and Najafi K 2006 Noise analysis and characterization of a sigma-delta capacitive microaccelerometer *IEEE J. Solid-State Circuits* **41** 352–61

Law W and Afromowitz M 2000 Noise-tolerant switched-capacitor time-delay measurement system for micro-fluidic flow sensing *Proc. ISCAS (Geneva)* pp 323–6

Lee J, Goericke F and King W P 2008 Temperature-dependent thermomechanical noise spectra of doped silicon microcantilevers *Sensors Actuators* A **145–146** 37–43

Lee S and Nguyen C T C 2003 Influence of automatic level control on micromechanical resonator oscillator phase noise *Proc. IEEE Int. Frequency Control Symp.* pp 341–9

Leland R P 2005 Mechanical thermal noise in MEMS gyroscope *IEEE Sensors J.* **5** 493–500

Levinzon F A 2004 Fundamental noise limit of piezoelectric accelerometer *IEEE Sensors J.* **4** 108–11

Li J, Xue M, Lu Z, Zhang Z, Feng C and Chan M 2003 A high-density conduction-based micro-DNA identification array fabricated with a CMOS compatible process *IEEE Trans. Electron. Devices* **50** 2165–70

Lin Q and Stern P E 2002 Analysis of a correlation filter for thermal noise reduction in a MEMS gyroscope *Proc. 34th Southeastern Symp. on System Theory* pp 197–203

Liu C H, Barzilai A M, Reynolds J K, Partridge A, Kenny T W, Grade J D and Rockstad H K 1998 Characterization of a high-sensitivity micromachined tunneling accelerometer with micro-g resolution *J. Microelectromech. Syst.* **7** 235–44

Liu C and Kenny T W 2001 A high-precision, wide-bandwidth micromachined tunneling accelerometer *J. Microelectromech. Syst.* **10** 425–33

Maluf N 1999 *An Introduction to Microelectromechanical Systems Engineering* (Boston, MA: Artech House)

McGill R A, Chung R, Chrisey D B, Dorsey P C, Matthew P, Piqu A, Mlsna T E and Stepnowski J L 1998 Performance optimization of surface acoustic wave chemical sensors *IEEE Trans. Ultrason. Ferroelectr. Freq. Control* **45** 1370–80

McLoughlin N, Lee S L and Hähner G 2007 Temperature dependence of viscosity and density of viscous liquids determined from thermal noise spectra of uncalibrated atomic force microscope cantilevers *Lab Chip* **7** 1057–61

Mohd-Yasin F, Korman C E and Nagel D J 2003 Measurement of noise characteristics of MEMS accelerometers *Solid-State Electron* **47** 357–60

Mohd-Yasin F, Nagel D J, Korman C E, Ong D S and Chuah H T 2007 Low frequency noise measurement and analysis of capacitive micro-accelerometers *Microelectron. Eng.* **84** 1788–91

Mohd-Yasin F, Nagel D J, Korman C E, Ong D S and Chuah H T 2008 Low frequency noise measurement and analysis of capacitive micro-accelerometers: temperature effect *Japan. J. Appl. Phys.* **47** 5270–3

Q8 Mohd-Yasin F, Zaiyadi N, Nagel D J, Ong D S, Korman C E and Faidz A R 2009 Noise and reliability measurement of a three-axis micro-accelerometer *Microelectron. Eng.* at press

Monajemi P and Ayazi F 2006 Design optimization and implementation of a micro-gravity capacitive HARPSS accelerometer *IEEE Sensors J.* **6** 39–46

Nagel D J and Zaghloul M E 2001 MEMS: micro technology, mega impact *IEEE Circuits Devices Mag.* **17** 14–25

Neumann J J and Gabriel K J 2001 CMOS-MEMS membrane for audio-frequency acoustic actuation *Proc. IEEE Int. Conf. MEMS* pp 236–9

Nguyen C T C and Howe R T 1994 Design and performance of CMOS micromechanical resonator oscillators *Proc. IEEE Int. Frequency Control Symp* pp 127–34

Nguyen C T C and Howe R T 1999 An integrated CMOS micromechanical resonator high-Q oscillator *IEEE J. Solid-State Circuits* **34** 440–55

Nguyen N T and Wu Z 2005 Micromixers—a review *J. Micromech. MicroEng.* **15** 1–16

Nimal A T *et al* 2006 A comparative analysis of one-port colpitt and two-port pierce SAW oscillators for DMMP vapor sensing *Sensors Actuators* B **114** 316–25

Oropeza-Ramos L A, Kataria N, Burgner C B, Astrom K J, Brewer F and Turner K L 2008 Noise analysis of a tunneling accelerometer based on state space stochastic theory *Proc. Solid-State Sensors, Actuators and Microsystem Workshop (Hilton Head, South Carolina)* pp 364–7

Oysted K and Wisland D T 2005 Piezoresistive CMOS-MEMS pressure sensor with ring oscillator readout including aΔ-Σ analog-to-digital converter on-chip *IEEE Custom Integrated Circuits Conf. (2005)* pp 511–4

Ozbay A *et al* 2006 Magnetic-field dependence of the noise in a magnetoresistive sensor having MEMS flux concentrators *IEEE Trans. Magn.* **42** 3306–8

Palaniapan M, Howe R T and Yasaitis J 2003 Performance comparison of integrated z-axis frame microgyroscopes *IEEE Int. Conf. on MEMS* pp 482–5

Pannetier M *et al* 2005 Noise in small magnetic systems—applications to very sensitive magnetoresistive sensors *J. Magn. Magn. Mater.* **290** 1158–60

Pattnaik P K, Selvarajan A and Srinivas T 2005 Guided wave optical MEMS pressure sensor *Proc. Sicon./ 05* pp 122–5

Pelesko J and Bernstein D 2002 *Modeling MEMS and NEMS* (Boca Raton, FL: CRC Press)

Petkov V and Boser B E 2005 A fourth-order sigma delta interface for micromachined inertial sensors *IEEE J. Solid State Circuits* **40** 1602–9

Radhakrishnan S and Lal A 2002 Scalable microbeam flowsensors with electronic readout *IEEE J. Microelectromech. Syst.* **15** 1013–22

Radhakrishnan S and Lal A 2003 In-channel micromechanical drag flow sensor with electronic readout *Proc. IEEE Int. Conf. MEMS* pp 307–10

Rebeiz G M 2002a Phase-noise analysis of MEMS-based circuits and phase shifters *IEEE Trans. Microw. Theory Tech.* **50** 1316–23

Rebeiz G M 2002b *RF MEMS: Theory, Design, and Technology* (New York: Wiley-Interscience)

Rocha L A, Cretu E and Wolffenbuttel R F 2005 Measuring and interpreting the mechanical thermal noise in MEMS *J. Micromech. Microeng.* **15** S30–8

Rombach P, Mullenborn M, Klein U and Rasmussen K 2002 The first low voltage, low noise differential silicon microphone, technology development and measurement results *Sensors Actuators* A **95** 196–201

Sankaranarayanan J G and Mayaram K 2007 Noise simulation and modeling for MEMS varactor based RF VCOs *Proc. of IEEE ISCAS (New Orleans)* pp 2698–701

Santos H J 2002 *RF MEMS Circuit Design for Wireless Communications* (Boston, MA: Artech House)

Savran *et al* 2002 Fabrication and characterization of a micromechanical sensor for differential detection of nanoscale motions *IEEE J. Microelectromech. Syst.* **11** 703–8

Savran C A *et al* 2003 Microfabricated mechanical biosensor with inherently differential readout *Appl. Phys. Lett.* **83** 1659–61

Scheeper P R, Nordstrand B, Gullv J O, Bin L, Clausen T, Midjord L and Storgaard-Larsen 2003 A new measurement microphone based on MEMS technology *IEEE J. Microelectromech. Syst.* **12** 880–91

Senturia S D 2000 *Microsystem Design* (Dordrecht: Kluwer)

Seshia A A, Howe R T and Montague S 2002a An integrated microelectromechanical resonant output gyroscope *Proc. IEEE Int. Conf. MEMS* pp 722–6

Seshia A A, Palaniapan M, Roessig T A, Howe R T, Gooch R W, Schimert T R and Montague S 2002b A vacuum packaged surface micromachined resonant accelerometer *J. Microelectromech. Syst.* **11** 784–93

Shaposhnik A V *et al* 2005 Determination of gases by a combined study of the resistance and noise characteristics of semiconductor sensors *J. Anal. Chem.* **60** 369–72

Sharma M, Kannan A and Cretu E 2008 Noise based optimization and noise analysis for resonant MEMS structures *Proc. of Symp. on Design, Test, Integration and Packaging of MEMS/MOEMS*

Shcheglov K, Evans C, Gutierrez R and Tang T K 2000 Temperature dependent characteristics of the JPL silicon MEMS gyroscope *Proc. Aerospace Conf.* pp 403–11

Supino R N and Talghader J J 2002 Average optical power monitoring in micromirrors *IEEE J. Sel. Top. Quantum Electron.* **8** 12–8

Suzuki K, Takiguchi K and Hotate K 2000 Monolithically integrated resonator microoptic gyro on silica planar lightwave circuit *J. Lightwave Technol.* **18** 66–72

Talghader J J 2004 Thermal and mechanical phenomena in micromechanical optics *J. Phys. D: App. Phys.* **37** 109–22

Tamayo J 2005 Study of the noise of micromechanical oscillators under quality factor enhancement via driving force control *J. App. Phys.* **97** 055903

Thompson S C, LoPresti J L, Ring E M, Nepomucheno H G, Beard J J, Ballad W J and Carlson E V 2002 Noise in miniature microphones *J. Acoust. Soc. Am.* **111** 861–6

Tu Y *et al* 2002 Quantitative noise analysis for gene expression microarray experiments *Proc. Natl Acad. Sci. USA* **99** 14031–6

Tucker R S, Baney D M, Sorin W V and Flory C A 2002 Thermal noise and radiation pressure in MEMS Fabry–Perot tunable filters and lasers *IEEE J. Sel. Top. Quantum Electron.* **8** 88–97

van Peppen J C L and Klaassen K B 2006 A new approach to micromagnetic simulation of thermal magnetic fluctuation noise in magnetoresistive read sensors *IEEE Trans. Magn.* **42** 56–69

Vidybida A K, Usenko A S and Kukla A L 2005 Structural characteristics of gas sensor based on conducting polymer *J. Optoelectron. Adv. Mater.* **7** 2815–21

Vig J R and Kim Y 1999a Noise in microelectromechanical system resonators *IEEE Trans. Ultrason. Ferroelectr. Freq. Control* **46** 1558–65

Vig J R and Kim Y 1999b Noise in microelectromechanical system resonators *IEEE Trans. Ultrason. Ferroelectr. Freq. Control* **46** 1558–65

Wang Z Y *et al* 2005 Design and optimization of laminated piezoresistive microcantilever sensors *Sensors Actuators* A **120** 325–36

Wu W, Greve D W and Oppenheim I J 2007 Characterization and noise analysis of capacitive MEMS acoustic emission transducers *Proc. IEEE Sensors Conf.* pp 1152–5

Wu S, Lin Q, Yuen Y and Tai Y C 2000 MEMS flow sensors for nano-fluidic applications *Proc. IEEE Int. Conf. MEMS* pp 745–50

Xie H and Fedder G K 2003 Fabrication, characterization, and analysis of a DRIE CMOS-MEMS gyroscope *IEEE Sensors J* **3** 622–31

Yazdi N and Najafi K 2000 Performance limits of a closed-loop, micro-g silicon accelerometer with deposited rigid electrodes *Proc. Int. Conf. Microelectron* pp 313–6

Yazdi N, Najafi K and Salian A S 2003 A high-sensitivity silicon accelerometer with a folded-electrode structure *J. Microelectromech. Syst.* **12** 479–86

Yeh C and Najafi K 1997a Micromachined tunneling accelerometer with a low-voltage CMOS interface circuit *Proc. Int. Conf. Solid State Sensors and Actuators* pp 1213–16

Yeh C and Najafi K 1997b A low-voltage tunneling-based silicon microaccelerometer *IEEE Trans. Electron. Devices* **44** 1875–82

Yoon E and Wise K D 1992 An integrated mass flow sensor with on-chip CMOS interface circuitry *IEEE Trans. Electron. Devices* **39** 1376–86

Yoshida Y, Kakuma H, Asanuma H and Niitsuma H 2005 A linear model based noise evaluation of a capacitive servo accelerometer fabricated by MEMS IEICE *Elect. Exp.* **2** 198–205

Yuan Z, Liu B and Sheng G 1999 Sensitivity study of 40 Gb/In2 recording systems to the fluctuation of head-disk spacing *IEEE Trans. Magn.* **35** 2241–3

Zhao Y, Mao M, Horowitz R, Majumder A, Varesi J, Norton P and Kitching J 2002 Optomechanical uncooled infrared imaging system: design, microfabrication, and performance *IEEE J. Microelectromech. Syst.* **11** 136–46

Zuckerwar AJ, Kuhn TR and Serbyn RM 2003 Background noise in piezoresistive, electret condenser and ceramic microphones *J. Acoust. Soc. Am.* **113** 3179–87

Queries

(1) Author: The sense of the phrase 'write to write' is unclear. Please check.
(2) Author: Please check whether reference Yeh and Najafi (1997) should be changed to Yeh and Najafi (1997a), Yeh and Najafi (1997b) or both and Seshia *et al* (2002) should be changed to Seshia *et al* (2002a), Seshia *et al* (2002b) or both here and elsewhere in the text.
(3) Author: Please check whether reference Vig and Kim (1999) should be changed to Vig and Kim (1999a), Vig and Kim (1999b) or both here and elsewhere in the text.
(4) Author: Please check whether the edit made in the sentence 'The work conducted at . . . ' retains your intended sense.
(5) Author: Please check whether the edit made in the sentence 'It is observed that two noise . . . ' retains your intended sense.
(6) Author: Please check whether reference 'Nguyen and Wu 2005' is okay as set in the sentence 'The applications cover . . . '.
(7) Author: Please check reference Pannetier *et al* (2003) has been changed to Pannetier *et al* (2005).
(8) Author: Please provide missing information, if any, in reference 'Dahlmann and Yeatman 2002'
(9) Author: Please update reference Mohd-Yasin et al (2009).
(10) Author: Dec *et al* (1998), Gomri *et al* (2006), Jwang *et al* (1997), Korvink and Greiner (2002), Levinzon (2004), Nimal *et al* (2006) are not cited in the text. Please check.
(11) Author: Please provide the email address of the corresponding author.
(12) Author: Please be aware that the colour figure 6 in this article will only appear in colour in the Web version. If you require colour in the printed journal and have not previously arranged it, please contact the Production Editor now.

Reference linking to the original articles

References with a volume and page number in blue have a clickable link to the original article created from data deposited by its publisher at CrossRef. Any anomalously unlinked references should be checked for accuracy. Pale purple is used for links to e-prints at arXiv.